# An Evaluation of Laser Extraction for Stable Isotopic Analysis of Carbonate and Hydrous Minerals

A Thesis Submitted to the College of
Graduate Studies and Research
in Partial Fulfilment of the Requirements
for the Degree of Master of Science
in the Department of Geological Sciences
University of Saskatchewan
Saskatoon

By
Michael David Powell
1992

In presenting this thesis in partial fulfilment of the requirements for a Postgraduate degree from the University of Saskatchewan, I agree that the Libraries of this University may make it freely available for inspection. I further agree that permission for copying of this thesis in a any manner, in whole or in part, for scholarly purposes may be granted by the professor or professors who supervised my thesis work or, in their absence, by the Head of the Department or the Dean of the College in which my thesis work was done. It is understood that any copying or publication or use of this thesis or parts thereof for financial gain shall not be allowed without my written permission. It is also understood that due recognition shall be given to me and to the University of Saskatchewan in any scholarly use which may be made of any material in my thesis.

Requests for permission to copy or to make other use of material in this thesis in whole or in part should be addressed to:

Head of the Department of Geological Sciences
University of Saskatchewan
Saskatoon, Saskatchewan S7N 0W0

**ACKNOWLEDGEMENTS**

I would like to give special thanks to T. K. Kyser, Dave Pezderic, and all members of the Consortium (you know who you are).

**ABSTRACT**

High-energy laser ionization of geologic materials is a potential replacement for conventional stable isotope extraction techniques because the former requires less sample material, requires less sample preparation and, most importantly, may allow direct in situ analysis. The laser extraction process explored in this study uses a pulse, focused Nd:YAG laser to excite the surface of carbonate and hydrous minerals producing a plasma. The plasma subsequently cools and condenses to form stable gaseous species such as CO and $CO_2$ from carbonates or $H_2$ and $H_2O$ from hydrous minerals. These species may be cryogenically separated and analyzed to obtain their isotopic compositions.

$\delta^{13}C$ and $\delta^{18}O$ values of calcite, dolomite, rhodochrosite, and siderite have been determined in situ using the laser extraction system. These values are distinctly different from isotopic compositions determined using standard acid dissolution techniques. Ionization with the laser produces gases, mainly CO and $CO_2$, and minor solid residues. The relative yields of these gases and the corresponding $CO_2/CO$ ratios are different for each carbonate mineral analyzed. Isotopic analyses of combined CO and $CO_2$ are reproducible to ±1°/oo to ±2°/oo, respectively, for $\delta^{18}O$ and ±2°/oo to ±3°/oo, respectively, for $\delta^{13}C$. The $CO_2$ produced from laser ionization of carbonates is consistently enriched in $^{13}C$ and $^{18}O$ relative

to the CO.

A two-stage model is proposed to explain the variations in the isotopic compositions observed using data from the laser ionization of carbonates. In the first stage, the energy is absorbed by the mineral, with the quantity and isotopic composition of gas formed being largely a function of the concentration of transition metals which absorb the 1.064$\mu$m wavelength of the Nd:YAG laser. In the second stage, the relative isotopic compositions of CO and $CO_2$ are affected by kinetically controlled reactions in the cooling plasma.

$\delta$D values of amphibole, biotite, phlogopite, kaolinite, muscovite, carnallite, and fluid inclusions in halite also have been determined using the laser extraction system. The laser ionization system is used in place of the conventional induction heating technique to extract water <u>in situ</u> from minerals. The water is then converted to hydrogen gas through exposure to uranium at 850°C. Difficulties in the spectroscopic analysis of small quantities of hydrogen were circumvented by direct capillary inlet of hydrogen gas into the ion source and development of a standard working curve determined through repeated analysis of waters with known isotopic compositions.

All $\delta$D values of water from hydrous silicates and evaporites determined using the laser ionization process are depleted, by over 100 per mil in some cases, relative to values determined by conventional methods. Differences in $\delta$D

values obtained using the laser system compared with those from conventional analysis were greatest in samples with the more D-rich structural water relative to a $\delta D$ value of approximately $-200^{\circ}/_{oo}$, that of local atmospheric water.

Experiments using evaporite minerals with a wide range of hydrogen isotopic compositions, similar water contents, and similar chemical compositions clearly show absorbed atmospheric water contamination affects the $\delta D$ values determined by laser ionization. A pressed powder pellet of kaolinite exposed to water having a $\delta D$ value of $+1000^{\circ}/_{oo}$ yielded aberrantly high $\delta D$ values when analyzed with the laser system relative to previous laser ionization analyses of the sample, demonstrating that atmospheric water contamination of samples can occur over days. Finally, laser ionization of anhydrous olivine yielded water, presumably from the surface, with $\delta D$ values similar to local atmospheric water. Thus even minor amounts of surface absorbed water can effect the results significantly.

Isotopic results obtained using Nd:YAG laser extraction of C and O from carbonates and H from hydrous minerals demonstrate that interactions between the laser beam and various minerals are largely dependent on the chemical composition and structure of the mineral being analyzed. As with all micro-sampling techniques, special care must be taken to ensure that all components and potential contaminants are well constrained prior to sampling.

Although the Nd:YAG laser can deliver an extremely high radiant flux density to target surfaces, the wavelength of the Nd:YAG in the near infrared makes it a poor choice for laser ionization of silicates, hydrous silicates, carbonates, oxides and evaporite minerals because absorption of near infrared energy by these of minerals is very dependent on their trace chemical compositions.

**TABLE OF CONTENTS**

**TABLE OF CONTENTS (Cont.)**

TABLE OF CONTENTS (Cont.)

LIST OF FIGURES

**LIST OF TABLES**

# 1. INTRODUCTION

## 1.1 General Statement

Relative abundances of the stable isotopes of hydrogen, carbon, nitrogen, oxygen, and sulphur can yield important information about the physical conditions under which minerals form in a particular rock. However, stable isotopic analyses use fractions of powdered samples, in marked contrast to many other types of geochemical analyses where analyses are performed in situ. For example, the electron microprobe can determine major and minor element abundances, the ion probe can determine abundances of transition and rare earth elements with the added capability of determining isotopic ratios, and laser microprobes are routinely used for the study of noble gases in minerals.

To obtain in situ stable isotope analyses of mineral grains, several laboratories have developed and tested laser-assisted extraction systems. The system developed at the University of Saskatchewan incorporates a Nd:YAG laser focused onto a mineral contained in a sample chamber under vacuum and connected directly to a MAT 251 stable isotope mass spectrometer.

The project is divided into two parts. First, an evaluation of the laser system for carbon and oxygen isotopic analysis of carbonate minerals is presented, and this is followed by an evaluation of the laser system for the analysis of the hydrogen isotopic composition of hydrous minerals.

Conventional carbon and oxygen isotopic analysis of carbonates as established by McCrea (1950) involves dissolving approximately 10mg to 30mg of powdered sample in phosphoric acid at constant temperature to form $CO_2$ and a residual metal oxide, then determining the isotopic composition of the $CO_2$ which is related to the isotopic composition of the sample. The analytical precision of this technique for natural carbonates is 0.1°/oo for $\delta^{18}O$ and 0.05°/oo for $\delta^{13}C$ values. Smaller amounts of sample (approx. 1mg) can be analyzed by this method using a specialized digestion chamber having a direct inlet to the mass spectrometer. Although this is suitable for analyses of individual microfossils such as foraminifers, most carbonate analyses are performed on powder obtained from larger samples of megafossils, rinds of sedimentary cements, blocky diagenetic and metamorphic crystals, and vein carbonate associated with metalliferous and magmatic environments. However, many of these carbonates are isotopically heterogeneous, having fine-scale variations that reflect original and altered compositions (e.g. Carpenter and Lohmann, 1989) or differential fractionation of C and O isotopes for each crystal face (Dickson, 1991). Small amounts of powder may be obtained from natural materials by using a microdrill, but when drilling small regions or specific zones of carbonate from a rock, contamination by adjacent materials may be unavoidable. Moreover, in high-resolution studies, the specific area of sampling often can only be determined using

petrographic methods. Thus, the difficulty in accurately determining the region to be drilled and limitations on the size of the area sampled by the drill, place severe restrictions on the applicability of this method for fine-scale studies.

Isotopic measurement of carbonates using laser-assisted extraction offers a method of in situ analyses that, in theory, circumvents many of the problems of sample preparation and relatively large sample size required by conventional means.

Laser ionization uses photons to directly atomize the carbonate producing $CO_2$, CO, and residual solid compounds containing metal cations. Sample preparation, at most, requires a thick-section be made upon which the laser beam can be focused. The sample can be accurately positioned for analysis while viewing it inside the sample chamber. The minimum spatial resolution of the laser beam is approximately 25$\mu$m to 50$\mu$m which is significantly less than the minimum of approximately 100$\mu$m resolution obtained by sampling using mechanical methods.

Several carbonate minerals having known and varied isotopic compositions were analyzed using the laser-assisted extraction system at the University of Saskatchewan. To compare laser systems, the same minerals were analyzed using a $CO_2$ laser system at the University of Michigan. The results of these studies are discussed in a following section.

The conventional technique for determining D/H ratios of water samples was developed by Bigeleisen et al. (1952) and involves the quantitative reduction of $H_2O$ to $H_2$ by passing the water over uranium metal at 850°C. Friedman and Smith (1958) applied the uranium reduction technique to determine the hydrogen isotopic composition of water from hydrous minerals. This technique, modified by Kyser and O'Neil (1984), releases water from hydrous minerals and aqueous fluid inclusions via induction heating, converts the water to $H_2$ by passing it over uranium metal at 850°C, and the $H_2$ is then collected cryogenically on charcoal at -196°C. Analysis of hydrous minerals using this method typically has a precision of 3°/∞. To measure $\delta D$ values of hydrous minerals, approximately 30mg to 50mg of sample must be separated from the host rock and induction heated to about 1400°C for 20 minutes to release the structural water for analysis. Laser ionization replaces the inductive heating process by acting as a spot furnace when focused onto the mineral surface. As with carbonate analyses, laborious sample separation and potential sample contamination is essentially eliminated by in situ laser extraction of water from hydrous minerals. Amphibole, biotite, kaolinite, muscovite, phlogopite, carnallite, and fluid inclusions in halite were analyzed using laser-assisted extraction, the results of which will be discussed later.

The application of laser-assisted extraction to measure isotopic compositions offers the promise of a significant

advance in our ability to observe small-scale geological processes operating in the natural environment. However, our enthusiasm to use this technique must be tempered by the necessity to clearly understand the many complex processes that occur during laser ionization. Many tests using the laser technique on carbonate and hydrous minerals were performed at the University of Saskatchewan and, although these systems were considered to be straightforward, many procedural difficulties were encountered. These results demonstrate that a more complete understanding of laser-mineral and laser-plasma-mineral interactions and associated factors is required.

## 1.2 Previous Work

Dalrymple (1989) provides a review of laser-assisted extraction applied to the $^{40}Ar$-$^{39}Ar$ age dating method. These laser systems, first developed by Megrue (1967), consist of a continuous beam output argon-ion laser with a wavelength of 0.50$\mu$m used for sample ionization, a small volume extraction line for purification of gas samples, and a rare gas mass spectrometer. Generally, these systems can produce data equivalent in accuracy and precision to conventional methods on samples much smaller than are required for conventional systems. Laser ionization for $^{40}Ar$-$^{39}Ar$ age dating allows <u>in situ</u> analysis of mineral grains, multiple analyses of single grains, and greatly reduces the minimum grain size of minerals

that can be analyzed. Lasers are successful for this method because the laser energy can easily disrupt the crystal lattice resulting in release of non-bonded argon contained therein.

Sommer et al. (1985) used laser-assisted decrepitation in conjunction with capacitance manometric analysis to determine $H_2O/CO_2$ ratios of fluid inclusions in quartz. A pulsed Q-Switched ruby laser with an energy output from 0.1J to 1J at a wavelength of 0.694$\mu$m was used to decrepitate single or groups of fluid inclusions. The minimum diameter of laser ionization pits on sample surfaces was approximately 50$\mu$m and the minimum diameter of fluid inclusions for accurate determination of $H_2O/CO_2$ ratios was 25$\mu$m. This technique proved to be very successful provided the laser energy was not so great as to melt the mineral itself. The laser-assisted system has the advantage that single fluid inclusions can be decrepitated in situ, provided minimum size requirements are fulfilled, in contrast to conventional vacuum furnace decrepitation methods which will not discriminate between large individual inclusions and the frequently more abundant small fluid inclusions typically found in quartz grains.

The procedure used by Sommer et al. (1985) is quite simple. An inclusion is targeted and a single pulse of Q-Switched laser energy is impinged onto the sample decrepitating the inclusion. All that is required of the laser is that it must have a Q-Switched output mode to provide

short, high energy pulses to break but not ionize the sample, and the wavelength of the laser must be partially absorbed by the sample.

The first application of laser ionization to stable isotope analyses was reported by Franchi et al. (1986) and subsequently in Franchi et al. (1989). Two laser-assisted techniques were developed for light-element stable isotopic analysis. Firstly, a Nd:YAG Q-switched laser with a 12mW output and a wavelength of 1.064 m was used to section diamond into blocks 250$\mu$m to 500$\mu$m on a side. The diamond blocks were studied using cathodeluminescence and infrared techniques to determine if impurities were present in the diamond. Sectioned blocks, weighing from 100$\mu$g to 500$\mu$g, were combusted to form gases which were subsequently analyzed on a high sensitivity stable isotope ratio mass spectrometer. This laser-sectioning technique has been successfully used to investigate the isotopic compositions of carbon and nitrogen and the nitrogen concentrations in diamonds.

The second technique used a Nd:Glass non-Q-Switched pulsed laser with an output range of 0.1J to 5J and a wavelength of 1.064$\mu$m to ionize mineral samples in situ with a spatial resolution of 50$\mu$m to 100$\mu$m. Ionization of samples by the laser beam produces a plasma cloud above the laser pit created on the sample surface. The plasma cloud cools and forms stable gas species which can be analyzed with a stable isotope ratio mass spectrometer to determine the isotopic

compositions of the gases of interest. Presumably, the gases formed by ionization will be in isotopic equilibrium with the sample material or will be consistently fractionated relative to the isotopic composition of the sample such that a correction factor can be applied. Thus, the isotopic composition of the gas can be used to determine the isotopic composition of the sample.

Franchi et al. (1986, 1989) attempted to use the carbon and oxygen isotopic compositions of $CO_2$ formed by laser ionization of carbonate minerals to determine their carbon and oxygen isotopic compositions. Analysis of calcite and siderite using laser-assisted extraction did not produce results with the accuracy or precision of the conventional acid digestion method. In Franchi et al. (1986, 1989), $\delta^{13}C$ values of $CO_2$ formed from laser ionization of calcite were within $\pm 3^{\circ}/_{oo}$ of the expected value, but most of the carbon results were depleted in $^{13}C$ relative to the carbon isotopic composition determined by conventional methods. Franchi et al. (1989) suggested either atmospheric $CO_2$ trapped in or on the sample, or possibly organic matter within the sample as sources of $^{12}C$-rich contamination. $\delta^{18}O$ values of $CO_2$ formed from laser ionization of calcite were depleted in $^{18}O$ by $10^{\circ}/_{oo}$ to $25^{\circ}/_{oo}$ relative to the true oxygen isotopic composition of the sample. Franchi et al. (1989) proposed several potential causes for the observed $\delta^{18}O$ results such as atmospheric $CO_2$,

$O_2$, or $H_2O$ contamination or residual metal oxide formation in the plasma affecting the oxygen isotopic composition of the $CO_2$ in much the same way as metal oxide formation affects the oxygen isotopic composition of $CO_2$ using the conventional method. Using the same experimental techniques, $\delta^{13}C$ and $\delta^{18}O$ values of $CO_2$ formed from laser ionization of siderite were enriched in $^{13}C$ and $^{18}O$, relative to the true isotopic compositions of the sample (Franchi et al., 1986). Considering both the calcite and siderite results, these data were interpreted to imply that mineral specific fractionations were occurring between the sample carbonate and released $CO_2$ during the ionization process (Franchi et al., 1986).

Franchi et al. (1989) obtained reliable $\delta^{15}N$ measurements of the nitrogen isotopic composition of various minerals using their laser-assisted extraction system. All $\delta^{15}N$ values determined on a TiN standard were within $\pm 4^{\circ}/_{\infty}$ of the true $\delta^{15}N$ value of the standard material. This application of the laser-assisted extraction system was successfully applied to determining nitrogen concentrations and $\delta^{15}N$ values of several meteorite samples.

Franchi et al. (1986, 1989) found limited applicability of their laser-assisted extraction system to in situ stable isotope analysis of minerals because the accuracy and precision of conventional techniques were not achieved. They did realize that differential absorption of laser energy by

the minerals being analyzed was possibly affecting their results, and that the formation of CO in addition to $CO_2$ during laser ionization of carbonate minerals could also affect the results on carbonates.

The procedure used by Franchi et al. (1986, 1989) was to impinge single or multiple non-Q-Switched pulses onto the sample surface to produce $CO_2$. Many of the other laser techniques used this type of laser output, however some workers used either continuous output or Q-Switched output modes. There is no clear consensus among published procedures on the best laser type or operating conditions to use.

Jones et al. (1986) used a Nd:YAG laser to determine the isotopic composition of carbon and oxygen in carbonate minerals and the isotopic composition of sulphur in sulphide minerals. Apparently, the $\delta^{13}C$ and $\delta^{18}O$ isotopic compositions of $CO_2$ from laser ionization of carbonates and the $\delta^{34}S$ isotopic composition of $SO_2$ from laser ionization of sulphides in the presence of $O_2$ are "identical" to the isotopic compositions of the same gases obtained by thermal decomposition of the same mineral samples, although no details are provided.

Sharp (1990) developed a laser-assisted fluorination technique to extract $O_2$ from silicates and oxides in the presence of $BrF_5$ for determination of oxygen isotopic compositions. The laser-assisted fluorination technique

involves heating samples with a pulsed output mode, 20W $CO_2$ laser at a wavelength of 10.6$\mu$m in a fluorine-rich atmosphere.

The conventional fluorination method uses fluorine gas or an interhalogen fluoride ($BrF_5$ or $ClF_3$) to react with powdered silicate or oxide samples to produce $O_2$ which is converted to $CO_2$ and analyzed by isotope ratio mass spectroscopy (Baertschi and Silverman, 1951; Clayton and Mayeda, 1963; Borthwick and Harmon, 1982). Generally, 5mg to 30mg of mineral is reacted with fluorine in nickel tubes for approximately 12 hours at 600°C. Samples as small as 1mg can be analyzed with this method, however problems arise with samples smaller than this because hygroscopic NiF is commonly formed during external heating of the nickel bombs. Hygroscopic NiF may react with the sample or may contribute contaminant water to the reaction vessel causing variations in the measured isotopic composition of oxygen from the sample. Larger sample sizes are required to overwhelm the NiF problem.

Laser-assisted fluorination extraction is quite similar to the conventional method in principle, with the added benefits of reduced reaction time, reduced sample size, and elimination of problems caused by NiF. The laser-based method simply uses the laser beam as a spot furnace to heat the sample powder directly.

Sharp (1990) performed two types of laser-assisted extraction of oxygen from silicates and oxides, analysis of powdered samples heated in nickel cups, and <u>in situ</u> rock thick

section analyses. Powdered samples (approx. 2mg) are loaded into the sample chamber, which is fluorinated at a low $BrF_5$ pressure to remove absorbed water. The sample chamber is fluorinated again for the laser analysis and the samples are heated with the laser beam for 30s to 240s. Sharp (1990) reported that the $\delta^{18}O$ values of powdered minerals, other than feldspar, determined by the laser-assisted fluorination technique are in agreement (±0.2°/oo) with corresponding conventional results. Some of the yields from his experiments were lower than expected, however, this has no apparent effect on the isotopic results. $\delta^{18}O$ values of selected minerals analyzed in situ with the laser system were erratic. Results from in situ analyses, obtained with the laser operated in pulsed mode and focused to a 100$\mu$m spot, were enriched in $^{18}O$ by up to 7°/oo, whereas when the laser was operated in continuous mode more accurate results were obtained within 1.0°/oo of conventional results.

The laser was operated in pulsed mode using 100ms pulses for the powdered silicate analyses. The powder was slowly heated with the laser at 20% of full power, pulsed at a rate of 1kHz, the energy was increased by increasing the pulse rate until the powder glowed and the experiment was complete when the sample no longer incandesced. The in situ analyses were most successful with the laser operated in continuous mode at 20% of full power for 1s. Sharp (1990) did not discuss the differences in laser operating conditions between powdered and

in situ analyses or the differences in the precision of the two methods.

In a more recent study, Sharp (1992) used single 20ms to 70ms pulses from a 20W $CO_2$-laser at full power to ionize carbonate samples forming $CO_2$. $\delta^{13}C$ and $\delta^{18}O$ values of the $CO_2$ were determined and these values, although highly reproducible ($\pm 0.1^{\circ}/_{oo}$ in some cases), lacked accuracy relative to the true carbon and oxygen isotopic compositions of the sample. Sharp (1992) does not put forward any explanation for the observed results.

Mattey et al. (1992) applied the laser-assisted fluorination method of Sharp (1990) to determine the oxygen isotopic compositions of orthopyroxene, clinopyroxene, and garnet mineral inclusions in diamonds. The inclusions ranged from 20$\mu$g to 500$\mu$g in size.

Kelley and Fallick (1990) used a laser-assisted extraction technique to obtain $SO_2$ from sulphide minerals providing $\delta^{34}S$ analyses with a spatial resolution of 250$\mu$m and a precision of $\pm 0.25(1\sigma)^{\circ}/_{oo}$. This system used an argon-ion laser with a continuous output of 4W at wavelengths of 0.488$\mu$m and 0.514$\mu$m to ionize sulphide minerals in situ in an oxygen atmosphere. $\delta^{34}S$ values of $SO_2$ from ionization of sulphide minerals produced results consistently depleted in $^{34}S$ relative to values determined by the conventional combustion technique (Rafter, 1965). These depletions are apparently mineral

specific, and if correction factors are applied the precision and accuracy of the laser-assisted technique are equivalent to the conventional method. The corrections added were +0.3°/oo to 0.4°/oo for sphalerite, +0.9°/oo to 1.3°/oo for pyrite, +0.7°/oo for chalcopyrite, and +2.6°/oo for galena.

Kelley and Fallick (1990) propose that the reason for the fractionation of sulphur isotopes during laser ionization is because there are two competing reservoirs for sulphur, $SO_2$ formed by combustion of S with $O_2$, and sulphur containing compounds plating out onto the sample chamber from direct vaporisation and ejection of sulphide material by the laser beam. They have correlated the observed fractionations with the relative bond strength of the sulphide minerals using the Gibbs free energy of formation at 25°C for each mineral. Presumably, sulphide minerals with weaker bond strengths vaporize more efficiently so that material quickly adheres to the walls of the sample chamber leaving less time for the material to combust and form $SO_2$.

Crowe et al. (1990) also developed a laser-assisted extraction technique to obtain $SO_2$ from sulphide minerals giving accurate in situ $\delta^{34}S$ analyses with a spatial resolution of 100$\mu$m to 200$\mu$m and precisions ranging from $\pm 0.15 (1\sigma)$°/oo for pyrite, pyrrhotite, and sphalerite to $\pm 0.43 (1\sigma)$°/oo for galena and chalcopyrite. A Nd:YAG laser with a continuous beam output of 10W at a wavelength of 1.064$\mu$m was used to ionize

the sulphide mineral samples. Crowe et al. (1990), like Kelley and Fallick (1990), found that $\delta^{34}S$ values of $SO_2$ produced by laser ionization of various common sulphide minerals were depleted in $^{34}S$ relative to the true sulphur isotopic composition of the mineral. Additive correction factors for the system of Crowe et al. (1990) were -0.10°/oo for sphalerite, +0.06°/oo for pyrite, +0.20°/oo for chalcopyrite, +1.36°/oo for pyrrhotite, and +0.47°/oo for galena.

These correction factors are smaller than those of Kelley and Fallick (1990). Crowe et al. (1990) hypothesize that fractionation of the sulphur in the $SO_2$ relative to the mineral is due to S diffusion in the sample immediately surrounding the laser pit. Investigation of laser pits revealed the presence of S deficient zones concentrically rimming the pits so they suggest that solid-state S loss is the mechanism controlling the mineral specific correction factors.

Both Kelley and Fallick (1990) and Crowe et al. (1990) use continuous mode output laser beams to ionize sulphide minerals. The differences between the correction factors calculated by each group is probably due to differences in the absorption each sulphide mineral has of the two different wavelengths of laser light used. The application of laser ionization to determine $\delta^{34}S$ values of sulphide minerals in situ is the most uncontested laser-assisted method developed

to date.

The Institute of Energy Technology in Norway has developed a laser-assisted stable isotope extraction system which has produced the majority of published data on carbonate analyses using laser ionization methods. The first publication (Smalley et al., 1989) describes a technique that uses a Nd:YAG Q-Switched pulsed laser to ionize calcite and aragonite in situ to determine $\delta^{13}C$ and $\delta^{18}O$ values of the samples. This technique is very similar to the technique of Franchi et al. (1986, 1989). Similar to all of these laser-assisted methods, a plasma cloud is created above a laser pit created by the impinging laser beam and as the plasma cools it condenses to form stable gas species which can be analyzed with a stable isotope ratio mass spectrometer to determine the isotopic composition of the sample. Smalley et al. (1989) used powdered calcite and aragonite standards to test their system. Their results show that $CO_2$ is the only major gas phase formed from ionization of powdered calcite and aragonite, the $CO_2$ has the same $\delta^{13}C$ value as the sample carbonate within $\pm 0.2 (1\sigma)^{\circ}/_{oo}$ and the $\delta^{18}O$ value of the $CO_2$ is consistently depleted in $^{18}O$ relative to the sample by $1.7^{\circ}/_{oo}$ for calcite and by $2.55^{\circ}/_{oo}$ for aragonite, within $\pm 0.2 (1\sigma)^{\circ}/_{oo}$. Subsequent papers describing results from laser-assisted extraction of calcite and aragonite, published by the this group, refer to this technique. A later study, Dickson et al. (1990), reported that $CO_2$ from laser ionization of carbonate

samples had a precision of $\pm 0.2(1\sigma)^{\circ}/_{oo}$ for $\delta^{13}C$ values, and the $\delta^{18}O$ value of the $CO_2$ released required a correction factor of $1.7^{\circ}/_{oo}$ consistent with previous publications, but the precision of $\delta^{18}O$ had decreased to $\pm 0.4(1\sigma)^{\circ}/_{oo}$. In Dickson et al. (1991), the accuracy and precision of $\delta^{13}C$ values are the same, the accuracy of $\delta^{18}O$ values is the same provided the same correction factor is applied, but the precision of the $\delta^{18}O$ values is reported as $\pm 0.3(1\sigma)^{\circ}/_{oo}$ to $\pm 0.4(1\sigma)^{\circ}/_{oo}$. Smalley et al. (1992) have since built another laser-assisted stable isotope extraction system nearly identical to the system in Norway and they report a new correction factor for $\delta^{13}C$ values of $CO_2$ formed by laser ionization of carbonate samples of $-0.8^{\circ}/_{oo}$ and a new correction factor for $\delta^{18}O$ values of $+1.2^{\circ}/_{oo}$. The reproducibility of these values are $\pm 0.2(1\sigma)^{\circ}/_{oo}$ for $\delta^{13}C$ values and $\pm 0.4(1\sigma)^{\circ}/_{oo}$ for $\delta^{18}O$ values.

Smalley and his associates are the major proponents for laser-assisted isotopic analysis of carbonates. However, close scrutiny of their data reveals some inconsistencies. Firstly, they use powdered standards to calculate their correction factors, but as will be shown in this study, there are substantial differences in results obtained with powdered versus in situ laser analyses. Secondly, they seem to be constantly modifying their correction factors and the precision of their results. Thirdly, they have never attempted to take into account or discuss the effect of the

chemical compositions of their carbonate samples or standards on the isotopic results from laser-assisted analyses, an effect that has been observed and documented in laser-assisted analyses of sulphides (Kelley and Fallick, 1990; Crowe et al., 1990) and in laser-assisted analysis of carbonates (Powell and Kyser, 1991).

Much of the published literature tends towards the application of laser ionization to determine the stable isotopic compositions of various minerals in geological systems, even though considerable discrepancies exist between values obtained using lasers and those measured conventionally. To accommodate these discrepancies, many workers simply apply poorly understood correction factors to their data rather than attempting to isolate the processes and factors that effect the measured isotopic compositions. The aim of this research is to understand the nature of laser-mineral and laser-plasma-mineral interactions, and the effects these interactions have on the stable isotopic compositions of laser-produced gases released during laser-assisted, in situ analyses.

## 2.0 METHODS

Determining the processes that occur during laser ionization of geologic materials for stable isotope analysis requires a clear understanding of the experimental procedures involved. The following is a brief overview of laser theory and a detailed description of the laser-assisted extraction system including the various components and procedures used to measure the carbon and oxygen isotopic compositions of carbonate minerals and the hydrogen isotopic composition of hydrous minerals.

During the design and construction of the laser ionization system at the University of Saskatchewan, a paucity of information existed on similar systems. Few details were available on the technical and operational aspects of laser systems as applied to geological samples, and much of the technical knowledge gained during the early stage of this project was through trial and error.

### 2.1 Lasers (Overview)

Laser is an acronym for "light amplification by stimulated emission of radiation". Lasers generate light that is unidirectional, coherent, and monochromatic, making them useful for high energy operations like the ionization (ablation) of minerals (Svelto, 1982). When an atom or a molecule undergoes an energy transition, that energy change will be a constant value for a specific transition. Lasers

utilize this property by making a large group of atoms or molecules undergo a specific energy transition producing photons of the same wavelength, which are coherent, and travelling in the same direction, which is by definition laser light. Generally, lasers operate using electronic energy level transitions to produce laser photons by exciting electrons in the active atoms (e.g. Cr in Ruby, Nd in Nd:YAG) to high energy orbitals then letting the atoms decay back to a lower or ground state, although some lasers (e.g. $CO_2$-lasers) use changes in vibrational and rotational energy levels.

Transitions from one electronic energy level to another occur when atoms absorb or emit photons. When an atom decays from an excited state to a ground state a photon will be emitted of a specific energy at a specific wavelength. Spontaneous emission is when the decay process occurs spontaneously. Photons released by spontaneous emission will stimulate other atoms in an excited state to decay releasing photons. This process is stimulated emission and it is a basic principle for generating laser light.

Lasers require a three or four level energy system to work. The lowest energy level is the ground state which is the most stable and is the energy atoms have in an unexcited state. The highest energy level in the system is commonly referred to as the pumping band and it is usually relatively unstable so atoms only remain at this energy level for a short

time (ns). Atoms of the active medium of the laser are excited to the pumping band energy level by absorbing photons of a specific energy, normally provided by an optical (flash lamp) or electrical (electric discharge) source. The final two levels make up the upper and lower energy levels of the lasing transition, and in a three level system the lower energy level of the lasing transition is the ground state. The upper lasing energy level is metastable relative to the other energy levels, excluding the ground state and electrons in this state will remain there for a proportionally long time (approximately 230$\mu$s for Nd:YAG lasers). As atoms in the active medium decay, through the process of stimulated emission, from the upper to the lower lasing energy levels photons are emitted. Once the atoms are in the lower lasing energy level they quickly decay back to the ground state to be excited up to the pumping band again. Because of the relative stability of the upper lasing energy level, a population inversion can be easily maintained.

There are many different types of lasers commercially available, the most common being solid state, semiconductor, gas, and dye lasers. The most common types of gas lasers are $CO_2$ lasers, HeNe lasers, and argon-ion lasers and the most common types of solid state lasers are Nd:YAG, Nd:Glass, and Ruby lasers. The energy level scheme of the active atoms or molecules of each laser determines the potential power and output wavelength of the laser; whether it can operate in

continuous mode, pulsed mode, or Q-Switched mode is largely a matter of design and engineering, although some lasers are limited in their output modes. Often the available modes of operation of a particular laser are determined by the producers of the laser.

Common commercially available lasers generally range in their radiant energy output from milli-Joules to Joules. Most workers in the field of laser ionization of geologic materials quote the radiant flux or power (W) of the laser they are using. Both radiant energy and radiant flux are of limited usefulness for estimating the true energy imparted onto the sample surface. For purposes of ionization of solid samples, radiant flux density ($Wm^{-2}$) is a more accurate and useful unit, however, this quantity is difficult to estimate because it is dependant on the area to which the beam is focused, thus the energy or power output of the unfocused laser beam is usually reported in publications.

The radiant flux density can be increased by focusing the laser photons to a smaller area, which is independent of the laser itself, or by decreasing the time it takes for the photons to be delivered to the target area, which can be laser controlled. Q-Switched lasers make use of a Pockels cell which is an electro-optic component that rotates its plane of polarization in response to a changes in electric potential. Through use of a Pockels cell, Q-Switched lasers can store polarized photons in the optical cavity of the laser until a

very high threshold is reached and then release them, by changing polarization to match that of the laser photons, in a pulse of extremely short duration (ns) and extremely high power. Solid state lasers like the Nd:YAG are commonly available with Q-Switched capability thus they can deliver enormous energy when tightly focused onto a surface. This is the main reason the Nd:YAG laser was chosen for our laser system.

## 2.2 Laser System

A schematic representation of the laser ionization system (Fig. 1) shows the laser, sample chamber, laser window, laser mirror, and laser objective lens, all of which are mounted on a Nikon Optiphot microscope. These components represent the major optical elements used to direct the laser beam onto the sample surface. The schematic also shows the extraction lines used to prepare the gas samples for analysis and the inlet to the mass spectrometer.

A Quanta-Ray DCR-11 Pulsed Nd:YAG Laser is used in the isotope extraction system at the University of Saskatchewan. The crystal medium of this laser is neodymium-doped yttrium aluminium garnet (Nd:YAG), the active material being the neodymium atoms ($Nd^{3+}$). The laser light generated by Nd atoms has a wavelength of 1.064$\mu$m, which is in the near-infrared part of the electromagnetic spectrum. The unfocused beam of the Quanta-Ray DCR-11 Nd:YAG laser is 6.4mm in diameter and

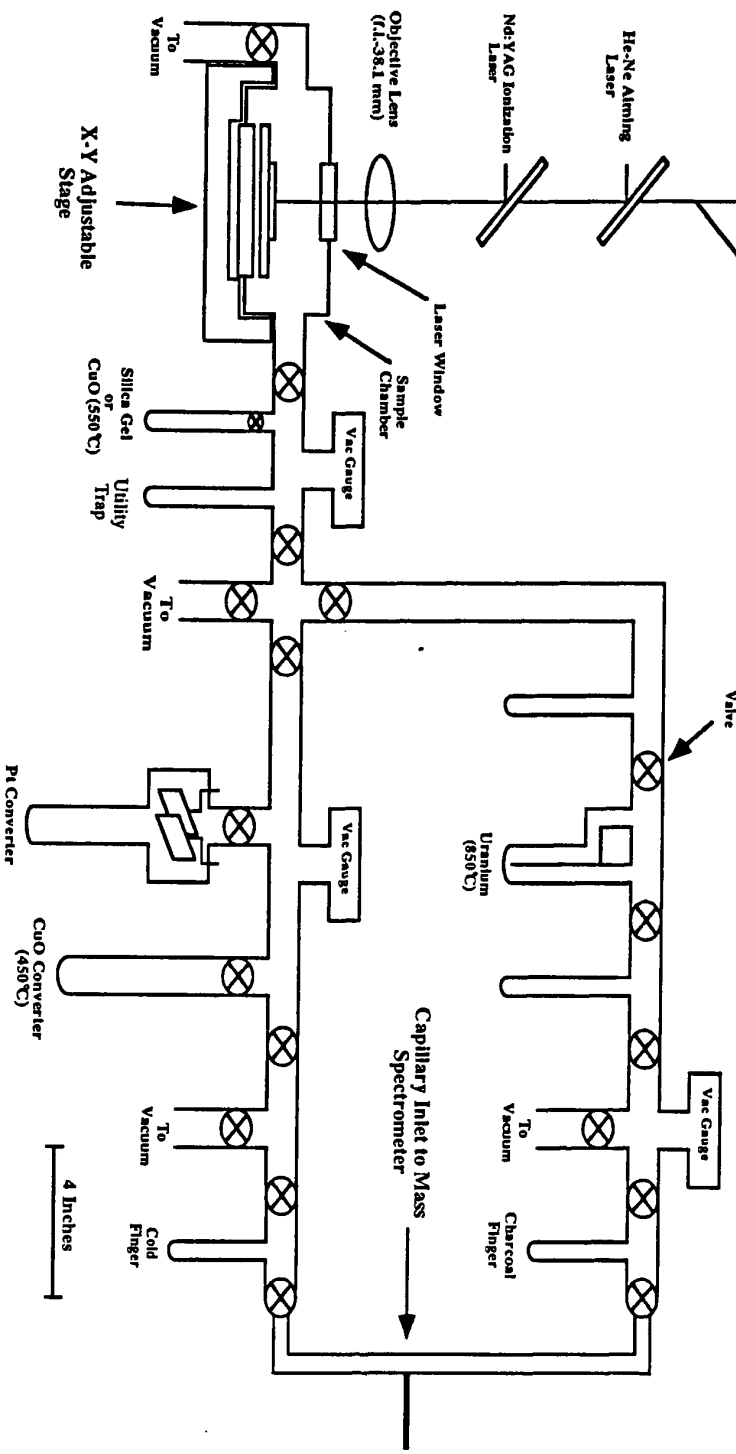


**Fig. 1. Schematic representation of the laser system, including the optic path and the extraction lines. The extraction lines were built with minimal volume for more efficient extraction of small samples.**

contains a maximum of approximately 500mJ of energy. The energy is released in a pulsed format only and can be controlled by varying the energy output of the arc-type flash lamp that pumps the active medium. The total range of energy output is from 0mJ to 500mJ, but typical energies used for ionization of samples were from 400mJ to 450mJ.

The Nd:YAG can be operated in long-pulse mode, in which the total pulse-energy is released over 200$\mu$s in a series of short pulses having durations of 8ns to 9ns with a separation between individual pulses of 2$\mu$s to 4$\mu$s. This mode produces a 200$\mu$s train of 50 to 100 energy spikes. The total power of a single pulse is in the range of thousands of Watts. Alternatively, in Q-switched mode, the total pulse-energy is reduced by approximately 10% relative to long pulse mode and is released in a single pulse only 2.5ns long. The total power of a Q-Switched mode pulse is in the range of hundreds of megaWatts. This particular model of Nd:YAG laser does not have continuous output mode capability. Nd:YAG lasers have a very stable output frequency so frequency variations are not a concern.

Carbonate analyses were acquired using long pulse mode as this evolves more gas from carbonates per pulse than does Q-Switched mode. Both modes impart sufficient energy onto sample surfaces to ionize the various carbonate minerals, but a 200$\mu$s long pulse can maintain ionization and plasma formation for much longer than a 2.5ns Q-Switched pulse.

Analysis of hydrous silicates to determine hydrogen isotopic compositions using long pulse mode to release the water from the samples left a relatively large quantity of melted material in and peripheral to the ionization pit (Fig. 2). Long pulse mode melted the samples rather than ionizing them, probably due to the long 200$\mu$s duration of the pulse. It was feared that the melt material would retain some of the water causing spurious results. Q-Switched laser pulses ionized rather than melted the hydrous silicate samples thus providing a more complete water sample from the area analyzed, however, the results did not improve. Various combinations of Q-switched and long pulse modes were tried, attempting to improve the precision of the results. Q-switched mode was used exclusively for the decrepitation of fluid inclusions in halite because it was desired to keep vaporisation of the mineral material itself to a minimum and only crack the sample (Sommer, 1985). Q-Switched mode was used for the carnallite analyses also.

The sample chamber is made of 316 stainless steel and is 10cm in diameter and 5cm high with a large sample loading port on the bottom and a laser window port on the top. The loading port consists of a 7cm Viton O-ring set into the body of the sample chamber covered with a glass plate held in place with a threaded brass ring. The inside of the sample chamber is threaded and holds a teflon sample holder which can be turned to adjust the distance of the sample from the laser window.

Figure 2. SEM photographs showing the effects of laser ionization on calcite and muscovite. (A) Calcite sample (MM) shows fracturing of the sample along cleavage planes peripheral to the pit and an abraded texture in the pit. There is no evidence of melting in this or any of the carbonate samples used in this study. (B) Muscovite sample (PMS) shows obvious melted material within and peripheral to the pit.

a

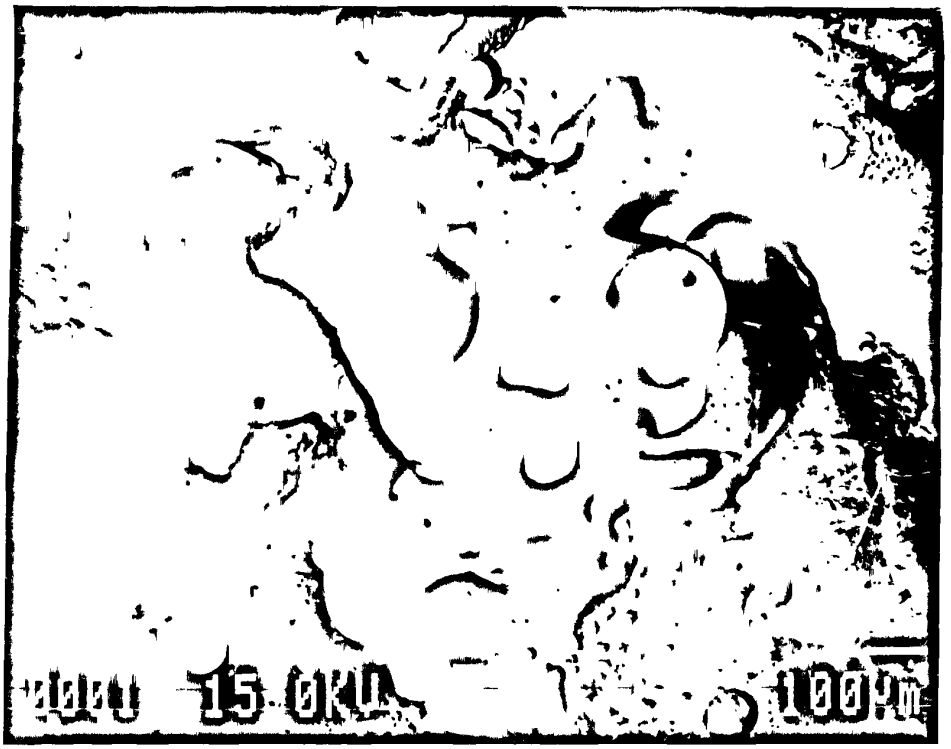

b

The sample, which is fixed to a standard petrologic microscope slide, is mounted on the teflon plate with two holding screws. Due to the constant ejection of material from laser pits during ionization experiments the distance from the sample surface to the base of the laser window was kept as great as possible for all experiments to prevent the ejecta from damaging the window. The top of the sample chamber has a 2.4mm Viton O-ring arrangement and threaded brass ring to hold the laser window in place and also to facilitate easy removal of the window for cleaning. Two Balzers quick release high vacuum flanges welded onto the body of the sample chamber provide connections to the vacuum pump and the extraction lines.

Gases generated by the ionization process in the sample chamber are collected cryogenically in the first utility trap and then are passed through either a hydrogen or a modified $CO_2/CO$ extraction line. Normal U-shaped cryogenic gas traps were replaced with single vertical tubes to reduce the overall volume of the extraction lines. The valves used in the extraction lines are Kontes Standard 4mm High Vacuum valves.

The extraction lines were designed to minimize internal volume by using 0.5mm (internal diameter) standard gas tubing. This is especially true for the inlet into the mass spectrometer where a gas sample expanded from either the cold or charcoal fingers progresses from glass capillary tubing (0.2mm internal diameter), into stainless steel capillary

tubing, then directly into the ion source of the mass spectrometer. This micro-inlet system provides adequate signals from small gas samples on the mass spectrometer, sufficient to acquire reliable results on gas samples ranging from 1$\mu$mol to 5$\mu$moles.

Internal vacuum line pressures are monitored with three DV-20 Teledyne Hastings-Raydist Thermal Conductivity vacuum gauge heads and a DV-6 Hastings Pressure Gauge. The vacuum pump used on this system is a TPH 060 Balzer Turbomolecular Pump backed with a two-stage rotary vane roughing pump, such that the system provides 30L/s volume flow rate capability and $1X10^{-8}$mbar final pressure. Temperatures of the uranium and copper oxide furnaces are monitored with Beckman Industries Type-K Thermocouple Thermometers. In addition, the extraction lines and sample chamber are wrapped with heating tape and held at 60°C to help facilitate transfer of small samples.

Gases produced during laser ionization of carbonate samples are introduced into a modified $CO_2$/CO extraction line which contains several specialized components. This extraction line is used to convert CO to $CO_2$ using firstly, a high voltage Pt converter that preserves the original $\delta^{18}O$ value of the CO by plating out carbon onto the Pt foils producing $CO_2$ (Aggett et al., 1965), and secondly a 450°C CuO converter that preserves the original $\delta^{13}C$ value of the CO by adding oxygen to the CO from the CuO to form $CO_2$. The Pt

converter was tested on CO from decomposed $CO_2$ of known oxygen isotopic composition by Longinelli and Craig (1967) and was found to convert the CO back to $CO_2$ to within ±0.1°/oo of the original oxygen isotope value. A single large sample of CO was converted to $CO_2$ several times using our Pt and CuO converters and the precision of the results was ±0.3°/oo for both $\delta^{18}O$ and $\delta^{13}C$ values. Because small samples of CO are difficult to convert to $CO_2$, it is estimated that these converters could introduce a maximum error of up to ±0.5°/oo in both $\delta^{13}C$ and $\delta^{18}O$ values. Gases produced during laser ionization of hydrous silicates and evaporite minerals are introduced into a conventional hydrogen isotope extraction line. Gases extracted from hydrous minerals are exposed to CuO, held at 550°C to enable complete conversion of hydrogenic gas species to $H_2O$, and collected in the utility trap. The temperature of the uranium is maintained at 850°C to facilitate reduction of small water-samples and once the water has been converted to $H_2$, it is collected in the charcoal finger at -196°C.

Samples can be viewed normally through the eyepieces of the microscope for focusing and positioning of the sample for ionization experiments. The laser extraction system has also been fitted with a video camera system which is routinely used to focus and position the samples. Long focal length universal stage microscope objectives were initially used to

focus the laser beam onto sample surfaces, but internal reflections of the laser beam caused these lenses to fracture and disintegrate. A 25mm diameter concave singlet Nd:YAG anti-reflection coated lens successfully replaced the high precision compound microscope objective lens. The simple nature of the laser optic elements means that the image of the sample has a limited resolution and finer details of the sample surface are often indistinct. Using the laser singlet lens, the total field of view that can be achieved with the eyepieces or the video system is approximately 500$\mu$m, and features on samples less than 50$\mu$m across are indistinct. Transmitted light is not useful for most of the samples analyzed with the laser system because the samples are normally thick sections or mineral chips. An external reflected light source is used to illuminate the sample surfaces by shining the light down through the laser window port. Laser pits of 25$\mu$m diameter can be achieved, although for routine analyses ionization pits are more commonly about 100$\mu$m to 200$\mu$m in diameter and about 500$\mu$m to 1mm deep (Fig. 2). The laser pits from routine analyses are easily discernable with the present optics.

**2.3 Sample Preparation**

Rock and pure mineral chips or prepared thick sections to be analyzed with the laser system are clamped or mounted onto a standard glass microscope slide in preparation for loading.

Samples were heated at 90°C in an oven for a minimum of three hours after the surfaces to be ionized were wiped with trichloroethane prior to loading the samples into the sample chamber. These treatments were used to remove surface absorbed contaminants which could possibly affect experimental results. Some of the samples which were uncut rock chips could not be effectively cleaned using these methods. Because of the limitations in optical resolution (50$\mu$m) once samples are in the sample chamber, appropriate ionization sites were sometimes mapped prior to loading to facilitate easy target location. Most of the samples were large homogeneous mineral chips or monomineralic thick sections so, as long as the samples were in focus, positioning was not difficult.

## 2.4 Extraction and Analytical Techniques for Carbonate Minerals

The only gaseous product of conventional phosphoric acid dissolution of carbonates is $CO_2$; using laser-assisted extraction, however, $CO_2$ is produced along with significant portions of CO, up to 70% CO in some cases. During analysis of the carbonate samples, gases produced by the ionization process are cryogenically collected at -196°C by adsorption onto silica gel in the first utility trap between the sample chamber and the extraction lines. Two types of carbonate experiments were performed. The first experiment determined the carbon and oxygen isotopic compositions of the $CO_2$ and CO.

The gases are initially separated by warming the silica gel trap to room temperature and exposing the gases to a trap at -196°C, which traps the $CO_2$. Then the CO can be recovered by recooling the silica gel trap to -196°C. The $CO_2$ can be analyzed directly by cryogenically moving it to the inlet cold finger and letting it into the mass spectrometer. The CO saved in the silica gel trap is expanded through a section of the $CO_2$/CO extraction line and divided into two isolated portions by closing a valve. The first portion of CO is converted to $CO_2$ with the Pt converter and the resultant $CO_2$, is analyzed but only the $\delta^{18}O$ value of the $CO_2$ is meaningful. Once the first portion has been analyzed and evacuated from the system the second portion of CO is exposed to the hot CuO converter and the resultant $CO_2$, is analyzed but only the $\delta^{13}C$ value of the $CO_2$ is meaningful.

The second type of experiment determined the $\delta^{13}C$ and $\delta^{18}O$ values of the $CO_2$ and CO together, not separated. Instead of initially separating the $CO_2$ from the CO the gases remain mixed and the procedures outlined for determination of $\delta^{13}C$ and $\delta^{18}O$ values of CO in the first experiment are followed. During the conversion of CO to $CO_2$ the $CO_2$ from laser ionization is cryogenically trapped prior to commencing the conversion process so that the original $CO_2$ will not be affected by the converters.

Typical quantities of $CO_2$, from mixed and unmixed

experiments, analyzed with the mass spectrometer using this system were 5$\mu$moles to 10$\mu$moles of $CO_2$, and accurate results required approximately 1$\mu$mole of $CO_2$.

Prior to analyzing $CO_2$ from laser-assisted extraction of carbonate samples, calibration of the capillary inlet of the laser system was necessary. $\delta^{13}C$ and $\delta^{18}O$ values of several $CO_2$ samples, encompassing a moderate range of carbon and oxygen isotopic compositions as determined through normal analyses were accurately reproduced when splits of these gas samples were introduced through the laser system capillary after appropriate adjustment of the capillary flow rate.

## 2.5 Extraction and Analytical Techniques for Hydrous Minerals

Most of the hydrogen released during isotopic analysis of hydrous minerals using the conventional induction heating technique is in the form of water. The laser ionization process, however, also produces significant quantities of molecular hydrogen and possibly HCl or HF. Therefore, gases extracted with laser ionization are exposed to CuO held at 550°C to enable complete conversion of hydrogenic gas species to $H_2O$. The temperature of the uranium is maintained at 850°C to facilitate reduction of small water-samples collected in the first utility trap from the sample chamber. Once the water has been converted to $H_2$, it is collected in the charcoal finger at -196°C. Typically 1$\mu$mol to 5$\mu$moles of $H_2$

were analyzed.

A procedure using two international isotope water standards V-SMOW and V-SLAP, and one well characterized in-lab isotope water standard UofS, encompassing a wide range of hydrogen isotopic compositions ($0^{\circ}/_{\circ\circ}$ to $-428^{\circ}/_{\circ\circ}$), was used to calibrate the hydrogen extraction section of the laser ionization apparatus and inlet system. When using the uranium reduction method of converting $H_2O$ to $H_2$ for hydrogen isotope analysis, a memory effect is normally observed. In this system, approximately 10% of the $H_2O/H_2$ is retained on surfaces of the uranium and this hydrogen can affect the isotopic composition of subsequent samples. The effect is especially pronounced if the isotopic composition of the later sample is distinctly different from the former sample. The procedure used to minimize the memory effect was to flush the uranium with a water having a hydrogen isotopic composition similar to the sample to be run or to run the sample twice consecutively discarding the first result. This procedure was necessary for calibration of the system with standards and, whenever possible, consecutive laser analyses of the same mineral sample were done to minimize memory effects.

Hydrogen isotopic compositions of standard waters determined using the laser extraction line are consistently enriched in D relative to compositions of standard waters prepared and let into the mass spectrometer in the conventional manner (Fig. 3). Because deuterium is double the

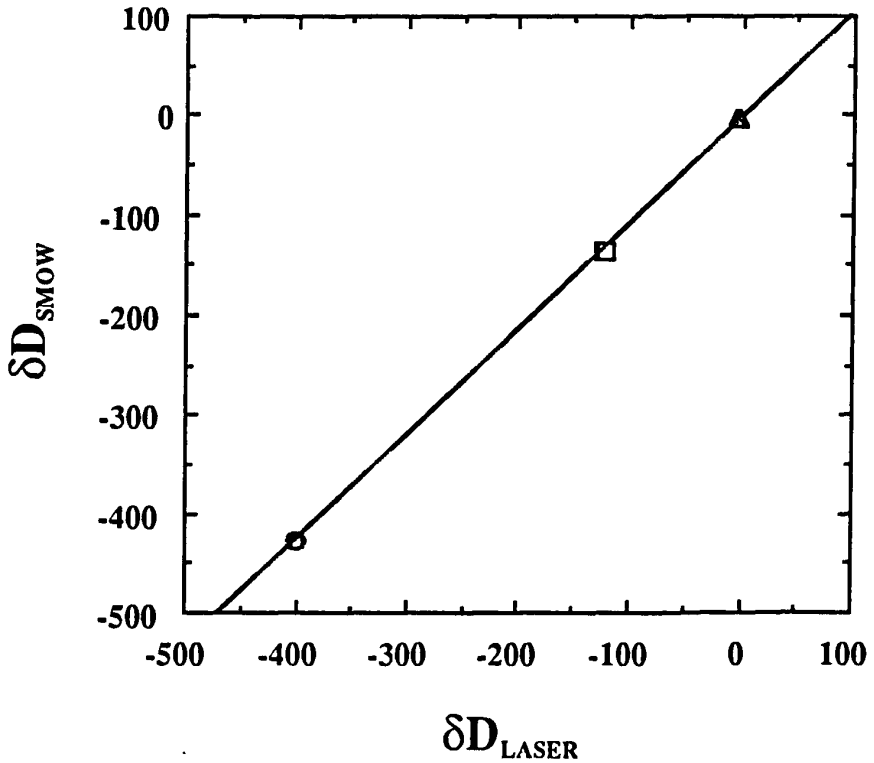


$$\delta D_{SMOW} = -3.32 + 1.1\ \delta D_{LASER}$$

Figure 3. Isotope calibration curve for conversion of hydrogen isotopic values determined through the laser capillary inlet system to known values determined conventionally; (○)=V-SLAP; (□)= UofS Std; (△)= V-SMOW.

mass of hydrogen, hydrogen gas is easily fractionated especially when passing through a restricted opening such as a mass spectrometer capillary. This is not a concern for normal isotopic analysis of hydrogen gas because the volumes, pressures, and the capillary flow rates of the sample and standard inlet systems are matched. For the laser inlet system, the sample gas originates from a volume different from the standard volume so that the pressure of the sample gas depletes at a different rate from the standard gas. Consistent isotopic results analyzed with the laser system hydrogen extraction line are achieved by balancing the laser inlet capillary and the standard gas inlet capillary so the gas signals deplete at the same rate. However, the pressures of the sample and standard gases in their respective reservoirs are not matched, thus requiring the corrections shown in Figure 3. This correction (or calibration) curve is valid for samples in excess of 0.1$\mu$L of $H_2O$ (Fig. 4).

The yield of $H_2O$ in microlitres ($\mu$L) from laser ionization of a mineral was estimated from the voltage of mass 2 and the use of a quantitative calibration curve (Fig. 4). This calibration curve was generated by analysis of standard water samples of known mass.

## 2.6 Definitions and Standard Notations

Stable isotope abundances are reported as delta ($\delta$) values in units of per mil ($^{o}/_{oo}$) as follows:

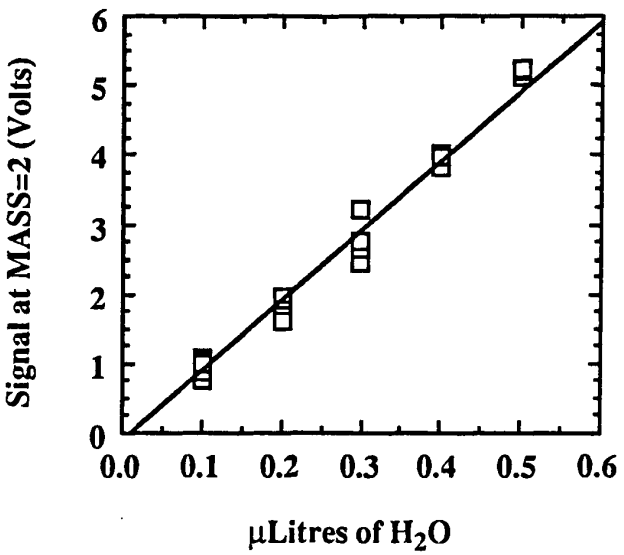


$$\mu L_{H_2O} = 0.01 + 0.1(\text{Volts})$$

Figure 4. Calibration curve for conversion of spectrometer signal of mass 2 in Volts to μLitres of $H_2O$, obtained by injecting known quantities of water; (□) denote data points.

$$\delta A\ (^{o}/_{oo}) = \{(R_A - R_{Stnd})/R_{Stnd}\} * 10^3.$$

$R_A$ and $R_{Stnd}$ are the absolute ratios of D/H, $^{13}C/^{12}C$, or $^{18}O/^{16}O$ in the sample and the standard, respectively. The isotopic compositions of $H_2$ and $CO_2$ from conventional and laser experiments are reported relative to V-SMOW for hydrogen and oxygen, and PDB for carbon.

# 3. RESULTS AND DISCUSSION OF CARBONATE ANALYSES

## 3.1 Results from Laser-Assisted Analyses of the Carbonate Samples

The majority of data presented are from experiments designed to identify the effects on the ionization process from variations in the characteristics of the laser-beam, different laser-sample and laser-plasma interactions, and sample morphology.

### 3.1.1 Results from Laser-Assisted Analyses of the Biogenically Formed Carbonate Sample (Mytilus Californianus)

Fine-scale isotopic zonation in carbonate shells and cements are of sufficient interest that laser ionization could provide additional information to more conventional stable isotope results. Sample PB, a primarily aragonitic fragment of the mollusc Mytilus californianus collected from Recent strata on the coast of California, represents the type of natural sample the laser was designed to analyze in situ. Mytilus californianus has variable oxygen and carbon isotopic variations in response to seasonal oceanic temperature variations and seasonal oceanic upwelling events (Killingley and Berger, 1979). Four large (approx. $2cm^2$) shell fragments were analyzed repeatedly using the laser ionization method. The laser was operated in long pulse mode at a pulse rate of 10 pulses per second during ionization of the shell fragments. Each analysis consisted of 10 to 20 separate laser pits.

Laser sampling was carried out normal to the growth lines of the shell to homogenize potential isotopic variations in a manner similar to that described by Muhs and Kyser (1987). The gases produced contained approximately equal amounts of CO and $CO_2$, and minor quantities of $H_2O$. The $H_2O$ probably originated from micro-inclusions in the aragonite or by oxidation of organic matter during ionization of the shell material. It should be noted that the gaseous products from ionization of the shell fragments were not cryogenically removed from the sample chamber during the experiment, the ramifications of which will be discussed later. Once enough gas had been generated, $CO_2$ was cryogenically transferred into the cold finger and admitted into the mass spectrometer for isotopic analysis. For these experiments, only the isotopic composition of $CO_2$ released by the laser beam impinging on the aragonite shell was measured.

The mollusc shell material has a bulk isotopic composition of $\delta^{13}C_{PDB}$=1.28±0.49(1$\sigma$)°/oo and $\delta^{18}O_{SMOW}$= 30.82±0.86(1$\sigma$)°/oo (Table 1), as determined by 11 analysis of 7 separate cut sections of 4 individual valves, using the standard acid-dissolution technique of McCrea (1950). Carbon and oxygen isotopic compositions of $CO_2$ from the mollusc shell as determined by 10 laser ionization analyses of 4 individual valves are much more variable and distinctly different from those of conventional analyses (Fig. 5). The average $\delta^{13}C$

Table 1

Laser-Assisted Analyses of Biogenic Carbonate

| Sample No. | L.E., Mode, Style | $\delta^{13}C_{PDB}$ | $\delta^{18}O_{SMOW}$ |
|---|---|---|---|
| PB-0(Std) | n.a. | 1.28 | 30.82 |
| PB-18 | 30, L.P., Grid | 0.08 | 27.06 |
| PB-19 | 30, L.P., Grid | -0.82 | 25.06 |
| PB-20 | 70, L.P., Grid | 1.57 | 26.61 |
| PB-21 | 60, L.P., Grid | 2.49 | 28.76 |
| PB-22 | 50, L.P.,Grid | 1.02 | 28.44 |
| PB-23 | 40, L.P., Grid | 3.36 | 27.10 |
| PB-24 | 65, L.P., Grid | -0.71 | 22.72 |
| PB-25 | 60, L.P., Grid | 5.35 | 23.68 |
| PB-26 | 55, L.P., Grid | 2.81 | 22.63 |
| PB-27 | 50, L.P., Grid | 4.21 | 25.10 |

PB=Punta Banda Mytilus californianus sample; (Std)=isotopic composition detemined by acid dissoloution; L.E.=lamp energy; Mode= laser operating mode (L.P.=long pulse); Style=ionization technique (Grid=multi-point ionization); n.a.=not applicable.

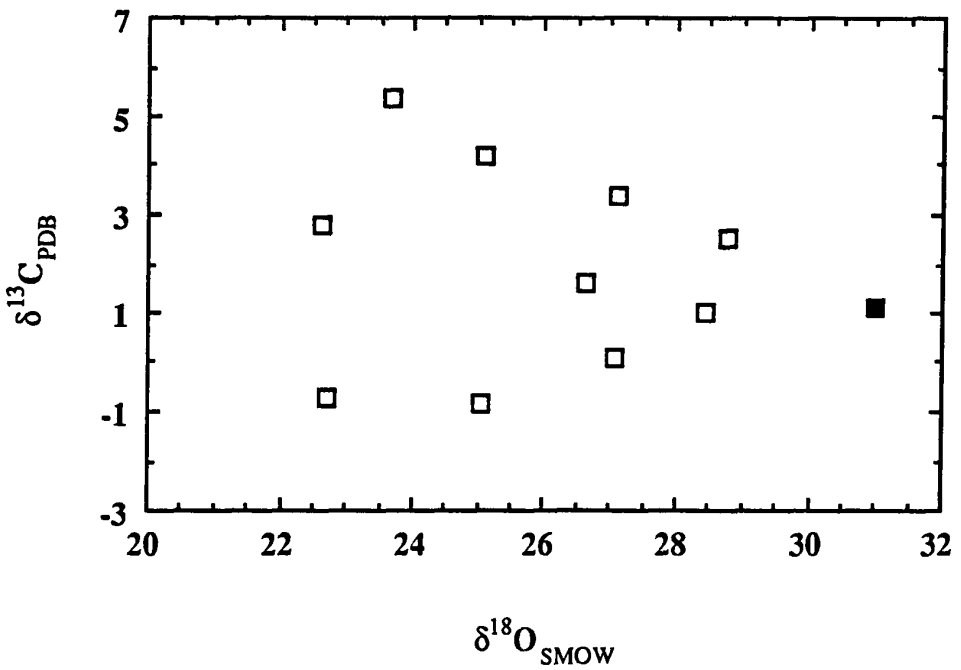


**Figure 5.** $\delta^{13}C$ and $\delta^{18}O$ vlaues of $CO_2$ from laser ionization (□) and conventional acid dissolution (■) of *Mytilus Californianus* Data from Table 1.

value determined using the laser technique is 1.94±2.08(1σ)°/₀₀ and the average $\delta^{18}O$ value is 25.72±2.23(1σ)°/₀₀.

These data clearly indicate that fractionations of carbon and oxygen isotopes between the mineral and the $CO_2$ produced during laser ionization are both variable and significant. Since CO was a major constituent of the gaseous ionization products, the previously described CO-$CO_2$ converters were added to the extraction line so that the carbon and oxygen isotopic compositions of both CO and $CO_2$ could be obtained. This was intended to provide further information on sample-laser interactions and the mechanisms controlling fractionations in the plasma.

### 3.1.2 Geological, Chemical, and Isotopic Data of the Inorganically Formed Carbonate Samples

Samples chosen for further testing of the laser extraction system were large, naturally formed crystals of inorganically formed carbonates. Calcite, dolomite, rhodochrosite, and siderite samples were used. A well consolidated marble (MM) collected from near Rutland Vermont was used as the calcite sample. Petrographically the marble contained calcite grains that averaged 0.5mm in diameter, showed good cleavage, abundant twinning, and a granoblastic texture. The dolomite sample (MD), from Thomwood, New York, had petrological features similar to the marble sample except that the average size of the dolomite grains was approximately

10mm. Electron microprobe analyses of these samples showed that they are essentially monomineralic. The siderite sample (MS) collected from Roxbury, Conneticut, had an average grain size 5mm and contained 5% interstitial quartz and limited alteration to fine-grained iron oxides along cleavage planes. The rhodochrosite sample (MR) from Sonora, Mexico, had an average grain size of 20mm and contained about 2% interstitial quartz and opaque minerals which occur in veins. The rhodochrosite was well-formed showing grains with well developed cleavage and some twinning.

As a test of their homogeneity the chemical compositions of the carbonates were determined using JEOL 8600 electron microprobe (Table 2), and several small fragments (<200mg) of each sample were analyzed for their isotopic compositions using standard acid dissolution (Table 3). Microprobe analyses indicated an overall chemical homogeneity of the carbonate standards although minor impurities such as quartz and opaque minerals are present in the rhodochrosite and siderite. Conventional isotopic analyses of each carbonate mineral were reproducible to $\pm 0.04 (2\sigma)^{\circ}/_{\circ\circ}$ for both carbon and oxygen (Table 3).

Laser ionization of samples was routinely carried out over a small area that resulted in a grid of closely spaced pits in the sample, a solid residue ejected from the laser pits including some cleavage fragments up to 0.25mm in length, and evolved CO and $CO_2$. The laser was operated in long pulse

Table 2

Chemical Analyses of Calcite (MM), Dolomite (MD), Rhodochrosite (MR), and Siderite (MS).

| | MM | MD | MR | MS |
|---|---|---|---|---|
| CaO | 59.00 | 32.98 | 0.34 | 0.49 |
| MgO | 0.60 | 23.38 | 0.80 | 3.16 |
| FeO | 0.06 | 0.12 | 0.08 | 56.31 |
| MnO | 0.07 | 0.00 | 67.05 | 4.16 |
| $CO_2$ | 40.28 | 43.52 | 31.73 | 35.89 |
| Total* | 100.01 | 100.00 | 100.00 | 100.01 |

* Normalized data

TABLE 3

Laser-Assisted Analyses of Inorganic Carbonates.

| Sample No. | L.E.,Mode,Style | Pulses | µmoles CO | µmoles $CO_2$ | $CO_2$/CO Ratio | $\delta^{18}O_{SMOW}$ | $\delta^{13}C_{PDB}$ |
|---|---|---|---|---|---|---|---|
| MM-0-#3(Std) | n.a. | | | | | 28.86 | 2.11 |
| MM-0-#4(Std) | n.a. | | | | | 28.82 | 2.11 |
| MM-0-#2(Std) | n.a. | | | | | 28.82 | 2.09 |
| MM-0-#1(Std) | n.a. | | | | | 28.87 | 2.11 |
| MM-0-#5(Std) | n.a. | | | | | 28.77 | 2.05 |
| MM-115(Comb) | 60, L.P., Grid | 210 | | | | | |
| MM-116(Comb) | 60, L.P., Grid | 240 | | | | 29.8 | 5.4 |
| MM-117(Comb) | 60, L.P., Grid | 200 | | | | 29.7 | 5.6 |
| MM-118(Comb) | 60, L.P., Grid | 200 | | | | 29.1 | 4.1 |
| MM-119(Comb) | 60, L.P., Grid | 220 | | | | 27.8 | 4.6 |
| MM-120(Comb) | 60, L.P., Grid | 180 | | | | 27.2 | 4.8 |
| MM-121(Comb) | 60, L.P., Grid | 220 | | | | 26.6 | 5.0 |
| MM-122(Comb) | 60, L.P., Grid | 220 | | | | 27.7 | 5.2 |
| MM-123(Comb) | 60, L.P., Grid | 200 | | | | 27.4 | 4.7 |
| MM-124(Comb) | 65, L.P., Grid | 200 | | | | 27.9 | 4.7 |
| MM-125(Comb) | 65, L.P., Grid | 200 | | | | 28.6 | 4.9 |
| MM-126(Comb) | 65, L.P., Grid | 200 | | | | 27.2 | 4.7 |
| MM-127(CO) | 60, L.P., Grid | 250 | 8.05 | 2.41 | 0.30 | 23.2 | 2.7 |
| MM-127(CO2) | | | | | | 26.9 | 4.3 |
| MM-128(CO) | 65, L.P., Grid | 225 | 9.00 | 2.36 | 0.26 | 24.8 | 3.4 |
| MM-128(CO2) | | | | | | 27.0 | 4.5 |
| MM-129(CO) | 65, L.P., Grid | 240 | 14.31 | 3.86 | 0.27 | 24.4 | 3.7 |
| MM-129(CO2) | | | | | | 27.6 | 4.7 |
| MM-130(CO) | 70, L.P., Grid | 225 | 11.10 | 2.91 | 0.26 | 25.3 | 3.9 |
| MM-130(CO2) | | | | | | 27.0 | 5.0 |
| MM-131(CO) | 60, L.P., Grid | 225 | 9.49 | 2.57 | 0.27 | 25.4 | 3.9 |
| MM-131(CO2) | | | | | | 26.8 | 4.8 |
| MM-132(CO) | 65, L.P., Grid | 225 | 10.16 | 2.87 | 0.28 | 26.1 | 4.0 |
| MM-132(CO2) | | | | | | 26.8 | 4.7 |
| MM-1(Mich/Comb) | Cont., Single Spot | | | | | 29.1 | 2.7 |
| MM-2(Mich/Comb) | Cont., Single Spot | | | | | 27.5 | 2.6 |
| MM-3(Mich/Comb) | Cont., Single Spot | | | | | 30.7 | 3.0 |
| MM-4(Mich/Comb) | Cont., Single Spot | | | | | 29.2 | 1.0 |
| MD-0-#2A(Std) | n.a. | | | | | 21.94 | 0.97 |
| MD-0-#1B(Std) | n.a. | | | | | 21.93 | 0.99 |
| MD-0-#2B(Std) | n.a. | | | | | 21.96 | 0.98 |
| MD-1(Comb) | 60, L.P., Grid | 150 | | | | 19.0 | -0.1 |
| MD-2(Comb) | 60, L.P., Grid | 225 | | | | 19.9 | 0.7 |
| MD-3(Comb) | 65, L.P., Grid | 225 | | | | 21.9 | 1.2 |
| MD-4(Comb) | 65, L.P., Grid | 180 | | | | 21.7 | 1.4 |
| MD-5(Comb) | 65, L.P., Grid | 150 | | | | 21.6 | 1.7 |
| MD-6(Comb) | 65, L.P., Grid | 180 | | | | 20.4 | 1.4 |
| MD-7(Comb) | 65, L.P., Grid | 150 | | | | 17.7 | 0.9 |
| MD-8(Comb) | 65, L.P., Grid | 180 | | | | 18.6 | 1.0 |
| MD-9(Comb) | 65, L.P., Grid | 180 | | | | 16.6 | 1.1 |
| MD-10(Comb) | 65, L.P., Grid | 180 | | | | 17.3 | 1.1 |
| MD-11(CO) | 65, L.P., Grid | 225 | 11.05 | 5.22 | 0.47 | 21.1 | 0.2 |
| MD-11(CO2) | | | | | | 24.3 | -0.1 |
| MD-12(CO) | 65, L.P., Grid | 225 | 9.07 | 3.49 | 0.39 | 21.2 | 0.5 |
| MD-12(CO2) | | | | | | 25.3 | 0.6 |
| MD-13(CO) | 60, L.P., Grid | 225 | 6.73 | 3.53 | 0.52 | 18.5 | 0.1 |
| MD-13(CO2) | | | | | | 24.4 | 0.5 |
| MD-14(CO) | 60, L.P., Grid | 225 | 7.74 | 2.86 | 0.37 | 18.1 | 0.5 |

MM=calcite; MD=dolomite; MR=rhodochrosite; MS=siderite; (Std)= isotopic composition determined by acid dissolution; (Comb)=isotopic compositions of CO and $CO_2$ determined together; (CO)=isotopiccomposition of CO only; ($CO_2$)=isotopic composition of $CO_2$ only; (Mich/Comb)=isotopic compositions of CO and $CO_2$ determined together using a $CO_2$-laser for ionization; L.E.= lamp energy; Mode= laser operating mode; Style= ionization technique; L. P.=long pulse; Grid=multi-point ionization style; Cont.=continuous ionization using $CO_2$-laser;unless otherwise specified, samples were analyzed using the Nd:YAG laser; n.a.= not applicable.

TABLE 3 (Cont.)

Laser-Assisted Analyses of Inorganic Carbonates.

| Sample No. | L.E.,Mode,Style | Pulses | µmoles CO | µmoles $CO_2$ | $CO_2$/CO Ratio | $\delta^{18}O_{SMOW}$ | $\delta^{13}C_{PDB}$ |
|---|---|---|---|---|---|---|---|
| MD-14(CO2) | | | | | | 23.0 | 1.4 |
| MD-15(CO) | 60, L.P., Grid | 225 | 9.96 | 3.31 | 0.33 | 19.6 | 0.6 |
| MD-15(CO2) | | | | | | 23.0 | 1.0 |
| MD-16(CO) | 65, L.P., Grid | 225 | 10.30 | 3.21 | 0.31 | 19.9 | 1.0 |
| MD-16(CO2) | | | | | | 24.1 | 1.8 |
| MD-17(CO) | 65, L.P., Grid | 225 | 13.39 | 4.34 | 0.32 | 18.8 | 0.8 |
| MD-17(CO2) | | | | | | 23.5 | 1.4 |
| MD-1(Mich/Comb) | Cont., Single Spot | | | | | 21.5 | 1.3 |
| MD-2(Mich/Comb) | Cont., Single Spot | | | | | 19.6 | 2.0 |
| MD-3(Mich/Comb) | Cont., Single Spot | | | | | 24.2 | 2.1 |
| MR-0-#1A(Std) | n.a. | | | | | 14.64 | -7.89 |
| MR-0-#1B(Std) | n.a. | | | | | 14.67 | -7.87 |
| MR-0-#2A(Std) | n.a. | | | | | 14.81 | -7.89 |
| MR-0-#2B(Std) | n.a. | | | | | 14.75 | -7.89 |
| MR-1(Comb) | 60, L.P., Grid | 200 | | | | 20.6 | -6.0 |
| MR-2(Comb) | 65, L.P., Grid | 200 | | | | 20.6 | -5.6 |
| MR-3(Comb) | 65, L.P., Grid | 200 | | | | 21.7 | -5.5 |
| MR-4(Comb) | 65, L.P., Grid | 200 | | | | 21.6 | -6.1 |
| MR-5(Comb) | 60, L.P., Grid | 150 | | | | 19.9 | -5.9 |
| MR-6(Comb) | 65, L.P., Grid | 150 | | | | 21.5 | -5.9 |
| MR-7(Comb) | 70, L.P., Grid | 150 | | | | 21.2 | -6.6 |
| MR-8(Comb) | 65, L.P., Grid | 90 | | | | 21.8 | -6.9 |
| MR-9(Comb) | 65, L.P., Grid | 90 | | | | 23.3 | -6.0 |
| MR-10(Comb) | 65, L.P., Grid | 90 | | | | 23.3 | -6.0 |
| MR-11(CO) | 60, L.P., Grid | 120 | 6.62 | 8.85 | 1.34 | 15.8 | -7.2 |
| MR-11(CO2) | | | | | | 21.9 | -5.0 |
| MR-12(CO) | 65, L.P., Grid | 130 | 7.12 | 11.02 | 1.55 | 15.0 | -7.3 |
| MR-12(CO2) | | | | | | 23.6 | -5.3 |
| MR-13(CO) | 70, L.P., Grid | 140 | 11.37 | 11.87 | 1.04 | 20.2 | -7.9 |
| MR-13(CO2) | | | | | | 23.6 | -5.4 |
| MR-14(CO) | 65, L.P., Grid | 140 | 5.77 | 10.00 | 1.73 | 19.7 | -7.8 |
| MR-14(CO2) | | | | | | 23.9 | -5.2 |
| MR-15(CO) | 65, L.P., Grid | 120 | 7.96 | 8.50 | 1.07 | 20.9 | -7.8 |
| MR-15(CO2) | | | | | | 23.4 | -5.5 |
| MS-0-#3(Std) | n.a. | | | | | 11.47 | -12.26 |
| MS-0-#1(Std) | n.a. | | | | | 11.50 | -12.28 |
| MS-0-#2(Std) | n.a. | | | | | 11.44 | -12.25 |
| MS-10(Comb) | 65, L.P., Grid | 240 | | | | 18.6 | -11.3 |
| MS-11(Comb) | 65, L.P., Grid | 100 | | | | 19.6 | -11.2 |
| MS-12(Comb) | 65, L.P., Grid | 120 | | | | 22.0 | -11.2 |
| MS-13(Comb) | 65, L.P., Grid | 120 | | | | 17.1 | -11.6 |
| MS-14(Comb) | 65, L.P., Grid | 120 | | | | 17.8 | -11.5 |
| MS-15(Comb) | 65, L.P., Grid | 140 | | | | | |
| MS-16(Comb) | 65, L.P., Grid | 140 | | | | 18.7 | -11.7 |
| MS-17(Comb) | 65, L.P., Grid | 175 | | | | 15.3 | -11.7 |
| MS-18(Comb) | 65, L.P., Grid | 100 | | | | 17.4 | -11.8 |
| MS-19(Comb) | 65, L.P., Grid | 175 | | | | 16.1 | -11.3 |
| MS-20(Comb) | 65, L.P., Grid | 120 | | | | 16.8 | -11.7 |
| MS-21(Comb) | 65, L.P., Grid | 120 | | | | 16.5 | -11.5 |
| MS-1(Mich/Comb) | Cont., Single Spot | | | | | 13.1 | -11.7 |
| MS-2(Mich/Comb) | Cont., Single Spot | | | | | 12.0 | -11.6 |
| MS-3(Mich/Comb) | Cont., Single Spot | | | | | 9.6 | -11.9 |

MM=calcite; MD=dolomite; MR=rhodochrosite; MS=siderite; (Std)= isotopic composition determined by acid dissolution; (Comb)=isotopic compositions of CO and $CO_2$ determined together; (CO)=isotopiccomposition of CO only; ($CO_2$)=isotopic composition of $CO_2$ only; (Mich/Comb)=isotopic compositions of CO and $CO_2$ determined together using a $CO_2$-laser for ionization; L.E.= lamp energy; Mode= laser operating mode; Style= ionization technique; L. P.=long pulse; Grid=multi-point ionization style; Cont.=continuous ionization using $CO_2$-laser;unless otherwise specified, samples were analyzed using the Nd:YAG laser; n.a.= not applicable.

mode at a pulse rate of 1 pulse per second during ionization of samples. Each analysis consisted of 15 to 25 separate laser pits with approximately 10 pulses impinged onto the sample surface to form each pit. No water was detectable in the gaseous products from the carbonate samples. Detailed examination of sample MM showed fracturing along cleavage planes peripheral to the pit and an abraded texture deeper into the pit (Fig. 2). No apparent melting occurred during laser ionization of any of the carbonates. Assessment of the laser extraction system for analysis of carbonates included determination of the yields of CO and $CO_2$, the individual $\delta^{13}C$ and $\delta^{18}O$ compositions of both gases, and the $\delta^{13}C$ and $\delta^{18}O$ compositions of both gases combined.

### 3.1.3 Relative Yields of CO and $CO_2$ from Laser-Assisted Analyses of the Carbonate Samples

The voltage corresponding to mass 44 ($^{12}C^{16}O^{16}O$) for each gas sample is directly proportional to the quantity of sample. By recording the initial voltages for mass 44 for the $CO_2$ and CO fractions, $CO_2$/CO ratios can be determined for experiments where the $CO_2$ and CO fractions are measured for their isotopic compositions separately. Of the carbonates studied, siderite and rhodochrosite yield the most gas during laser ionization (Table 3), indicating they absorb the laser beam more efficiently than dolomite or calcite (Fig. 6). In addition,

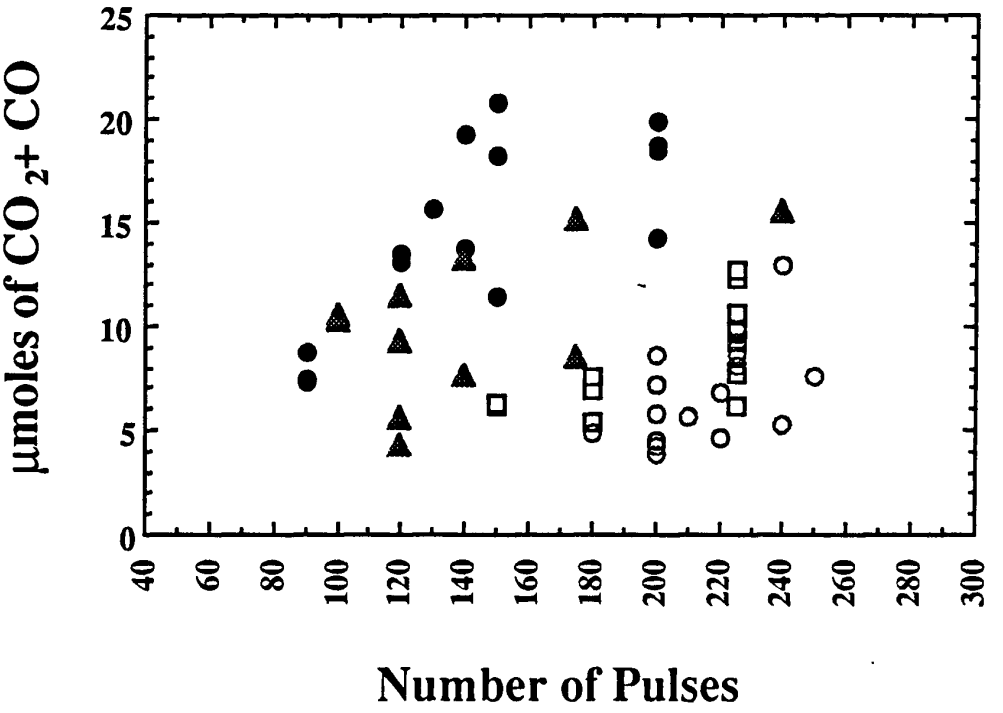


**Figure 6. Yields of total $CO+CO_2$ produced as a function of the number of pulses impinged onto the sample surface for different carbonate minerals during laser ionization; ○=calcite; □=dolomite; ●=rhodochrosite; ▲=siderite. Rhodochrosite and siderite yield greater quantities of gas per pulse than do calcite or dolomite.**

the ratio of $CO_2$ to CO released during laser extraction was different depending on the carbonate mineral being analyzed (Fig. 7). $CO_2$/CO ratios for rhodochrosite range from approximately 1.5 to 2.0, whereas $CO_2$/CO ratios of calcite and dolomite are approximately 0.4 and 0.6, respectively. These observations are independent of the number of pulses impinged onto the sample or the lamp energy used during the experiment.

### 3.1.4 Effects of Differential Gas Removal During Laser -Assisted Analyses

Removal of CO and $CO_2$ produced during laser ionization of calcite (MM) from the sample chamber results in variable $\delta^{13}C$ and $\delta^{18}O$ values of $CO_2$ because there is an interaction between the incoming laser beam and gases present in the sample chamber. The $CO_2$ and CO were removed during laser-assisted analyses of calcite (MM) in three different ways: (1) no gaseous products were removed during ionization, this was also the method employed for the Mytilus californianus analyses, (2) trapping only $CO_2$ from the chamber during ionization, by cryogenic removal at -196°C in the first utility trap, and (3) removing all gases produced during ionization by adsorption onto silica gel at -196°C in the first utility trap. The three methods yielded distinct isotopic compositions of $CO_2$ which was the only gas measured (Fig. 8), thus indicating that the laser energy was affecting the isotopic composition of

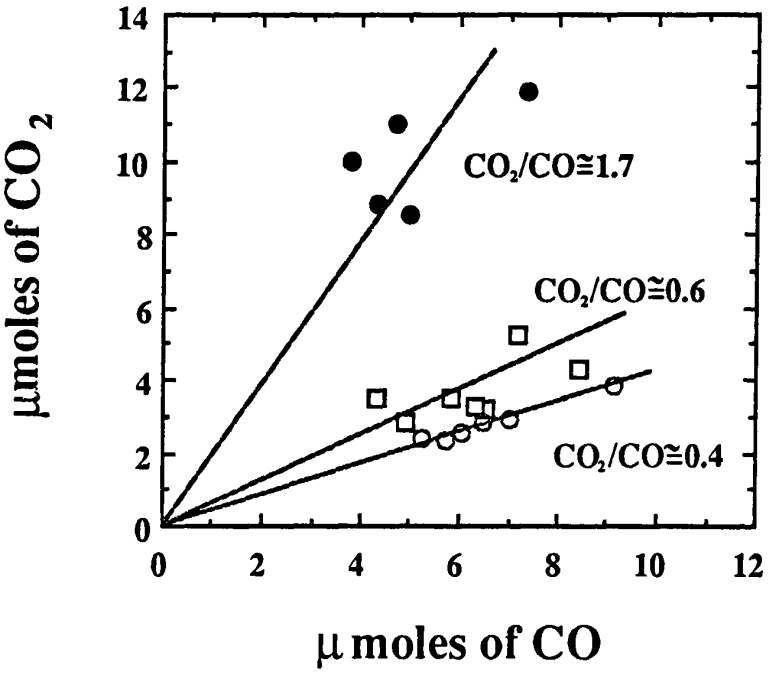


Figure 7. Ratios of $CO_2$ to CO produced during laser ionization of different carbonate minerals under conditions described in Table 3: ○=calcite, □=dolomite, ●=rhodochrosite. Rhodochrosite yields higher $CO_2$/CO ratios than calcite or dolomite.

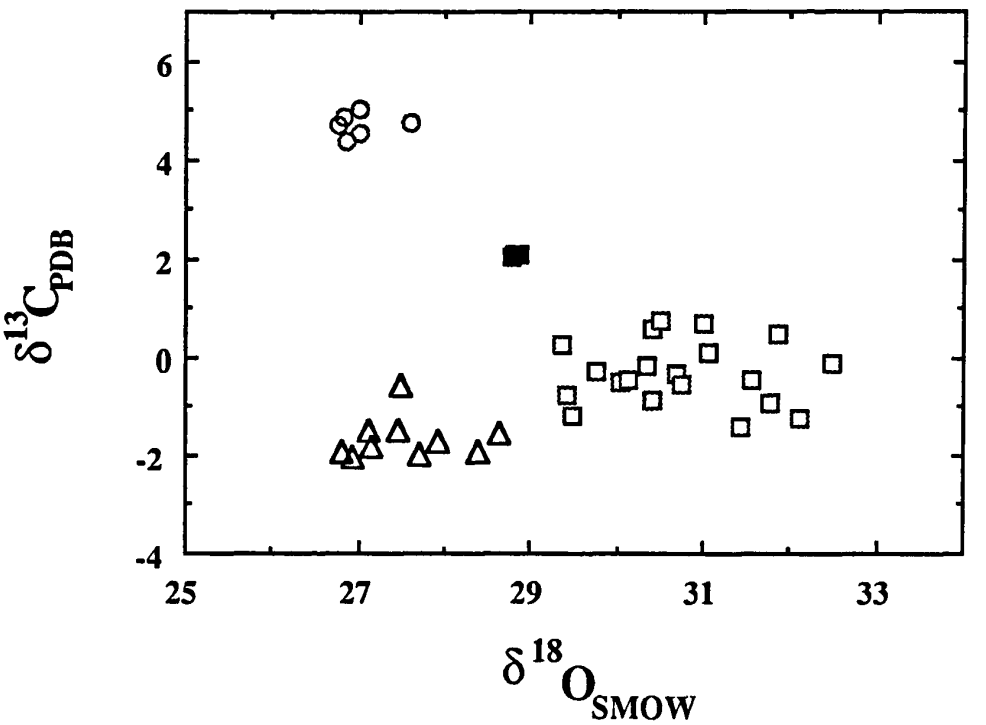


Figure 8. Effects of different gas removal schemes on the isotopic compositions of the $CO_2$ released from calcite sample (MM) during laser ionization : △= removal of no gaseous products during ionization; □= removal of $CO_2$ only during ionization; ○ = removal of all gaseous products during ionization. The isotopic composition of calcite sample (MM) determined by acid dissolution is also shown (■).

already formed $CO_2$ via interaction with the gas plume. Because removal of both CO and $CO_2$ produced more consistent results and minimized interactions between the gases released and the laser energy, all the gases were collected on silica gel at -196°C during laser ionization in all other experiments. This allowed most of the gas produced during one pulse to be collected before the next pulse, thus minimizing laser-gas interactions.

### 3.1.5 Results Using the Nd:YAG Laser

The CO and $CO_2$ released from the inorganic carbonate samples by the laser ionization process have $\delta^{13}C$ and $\delta^{18}O$ values that differ substantially from those obtained by acid dissolution (Fig. 9). Further, $CO_2$ is enriched in both $^{13}C$ and $^{18}O$ relative to CO for the majority of the inorganic carbonate samples (Fig. 9). The relative average enrichments in $\delta^{13}C$ and $\delta^{18}O$ of $CO_2$ relative to CO are 1.1°/oo in $\delta^{13}C$ and 2.2°/oo in $\delta^{18}O$ for calcite, 0.4°/oo in $\delta^{13}C$ and 4.3°/oo in $\delta^{18}O$ for dolomite, and 2.3°/oo in $\delta^{13}C$ and 4.9°/oo in $\delta^{18}O$ for rhodochrosite.

$\delta^{13}C$ and $\delta^{18}O$ values of combined CO and $CO_2$ from laser ionization of the inorganic carbonate samples were determined by splitting the mixed gas into two portions and converting the CO in each portion to $CO_2$ to conserve either the $\delta^{13}C$ or $\delta^{18}O$ value of the CO. The combined CO and $CO_2$ should represent all of the carbon and oxygen released from the sample, having

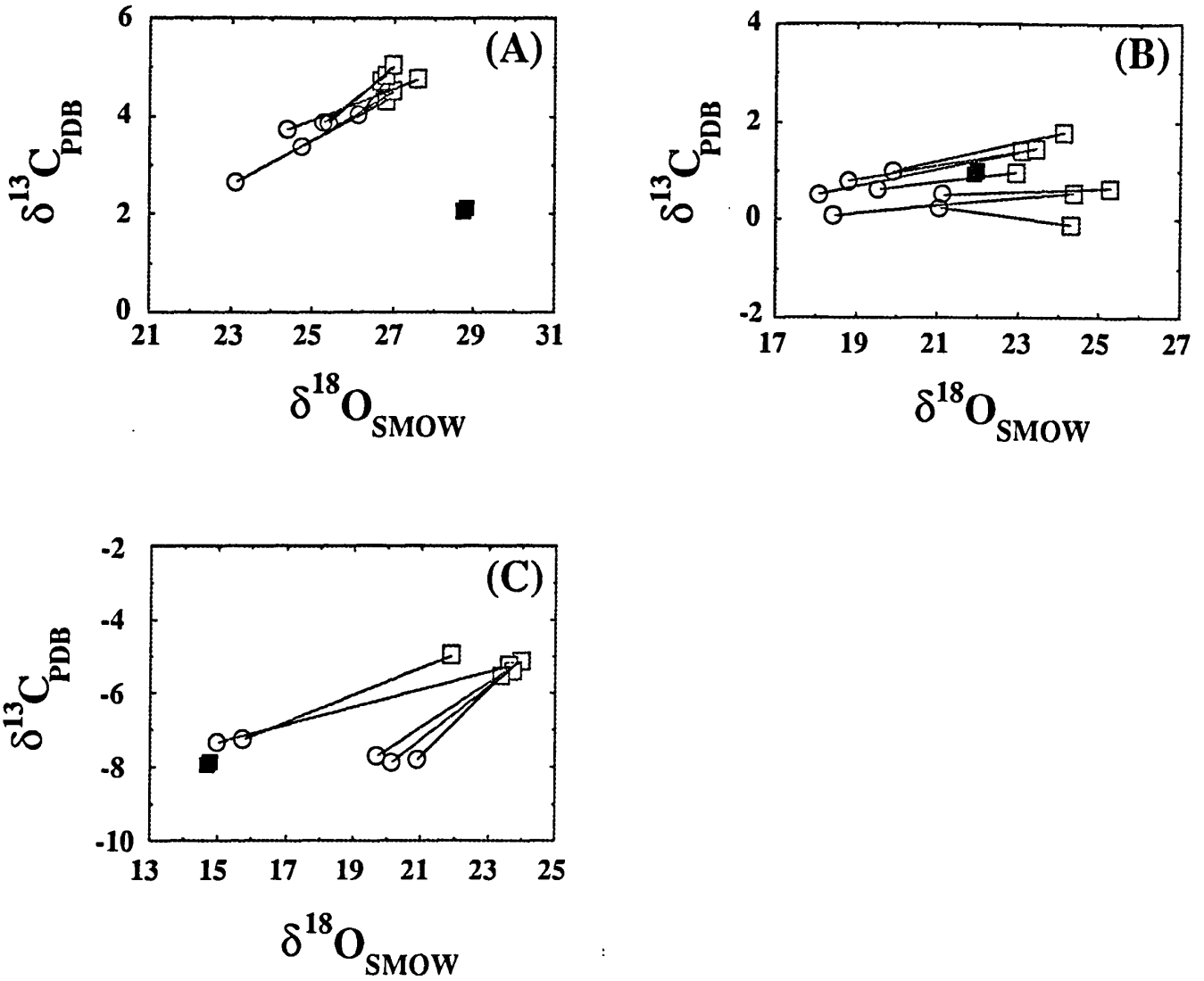


Figure 9. Isotopic compositions of CO (○) and $CO_2$(□) produced from the same experiment during laser ionization of different carbonate minerals: (A) calcite; (B) dolomite; (C) rhodochrosite. $CO_2$ is generally enriched in $^{13}C$ and $^{18}O$ relative to CO as indicated by the tie-lines which connect gases formed during the same experiment. The isotopic compositions of the carbonates determined by acid dissolution are also shown (■).

$\delta^{13}C$ and $\delta^{18}O$ values that theoretically represent the isotopic composition of the mineral being analyzed. Most of the carbonate results show the $\delta^{13}C$ and $\delta^{18}O$ values of the combined CO and $CO_2$ differ significantly from the values obtained with the conventional technique (Fig. 10).

### 3.1.6 Results Using the $CO_2$ Laser

The calcite, dolomite, and siderite samples used in this study also were analyzed using a $CO_2$ laser system developed by Dr. J. R. O'Neil at the University of Michigan. The experimental techniques used with the $CO_2$ laser were similar to those techniques employed with the Nd:YAG laser system. Gases, predominantly CO, produced through laser ionization with the $CO_2$ laser were removed from the sample chamber during ionization by absorption onto silica gel at -196°C, and the CO was converted using the same types of converters used on our system. The $CO_2$ laser differs from the Nd:YAG in that the wavelength of the $CO_2$ laser is 10.6$\mu$m. The $CO_2$ laser also operates in continuous mode rather than pulsed and the beam was not focused, producing laser pits approximately 1mm in diameter. The energy of the $CO_2$ laser produces heating rather than impact and ionization. This is supported by the melted textures of the laser pits and that spectroscopic studies show that most carbonate minerals at least partially absorb light at 10.6$\mu$m (Farmer, 1974). The carbon and oxygen isotopic

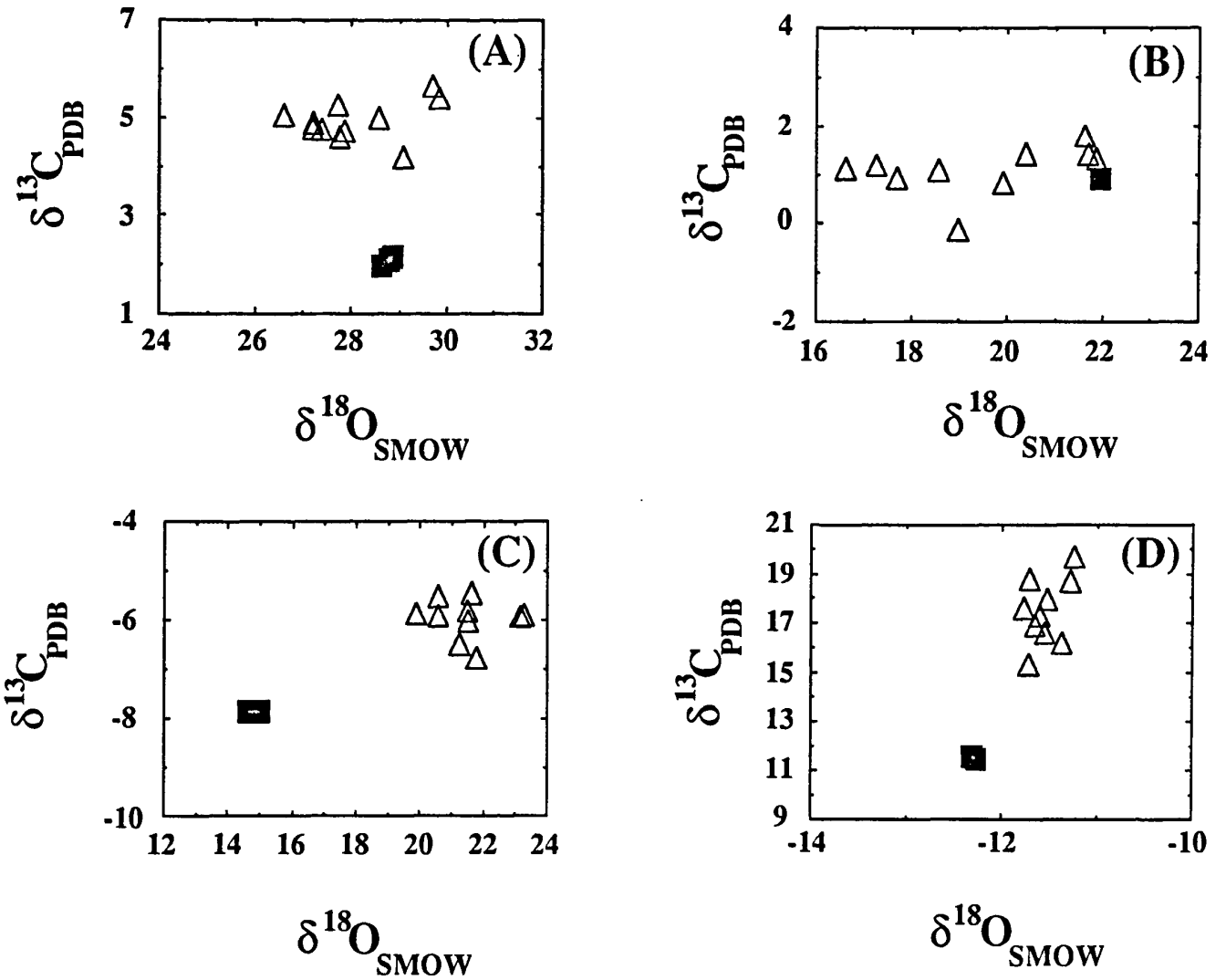


Figure 10. Isotopic compositions of combined CO and $CO_2$ ( Δ) produced during laser ionization by a Nd::YAG laser of different carbonate minerals: (A) calcite; (B) dolomite; (C) rhodochrosite; and (D) siderite. The isotopic fractionations between the combined gas and the mineral, as represented by the isotopic compositions determined by acid dissolution ( ■), is specific to the mineral being analyzed.

compositions of CO and minor $CO_2$ released from calcite, dolomite, and siderite have a range of values similar to those determined by Nd:YAG laser-assisted extraction, but the values are closer to the isotopic compositions determined by conventional methods (Fig. 11).

### 3.2 Discussion of the Carbonate Results

The data from analyses of the carbonates can be used to model the laser-mineral and laser-plasma-mineral interactions that occur during laser ionization. The model must explain why the quantities of CO plus $CO_2$ and the $CO_2$:CO ratios are higher in carbonates having high concentrations of transition metals, especially Fe. It should also account for the isotopic fractionations between CO and $CO_2$, and isotopic fractionations between the mineral and produced gases. Finally, the model should show why results differ for analyses obtained using a $CO_2$ laser rather than a Nd:YAG laser.

The model developed requires two distinct stages to explain the quantities of gases produced and their fractionations, and is constrained primarily by the data obtained via laser ionization of carbonates, although the model must also apply to the effects observed in analysis of hydrous minerals to be discussed later.

#### 3.2.1 Mineral Ionization Model

A two-stage model is proposed to explain results obtained

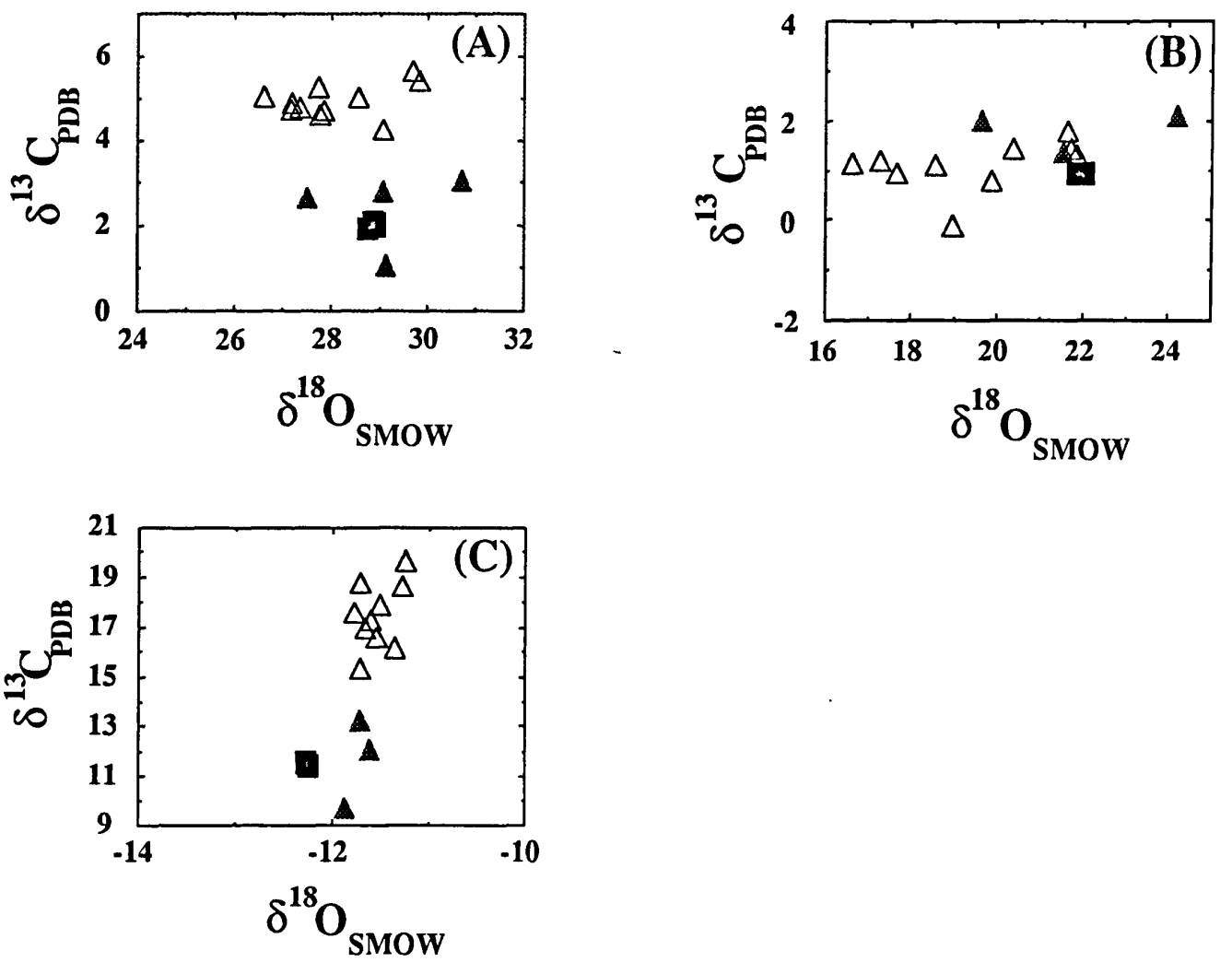


**Figure 11.** Isotopic compositions of combined CO and $CO_2$ produced during laser extraction of different carbonate minerals using a Nd:YAG ( Δ) and a CO2-laser ( ▲) : (A) calcite; (B) dolomite; and (C) siderite. $CO_2$ laser results are generally more accurate than Nd:YAG results; however, both techniques suffer from a lack of precision. The isotopic compositions determined by acid dissoloution are also shown ( ▩).

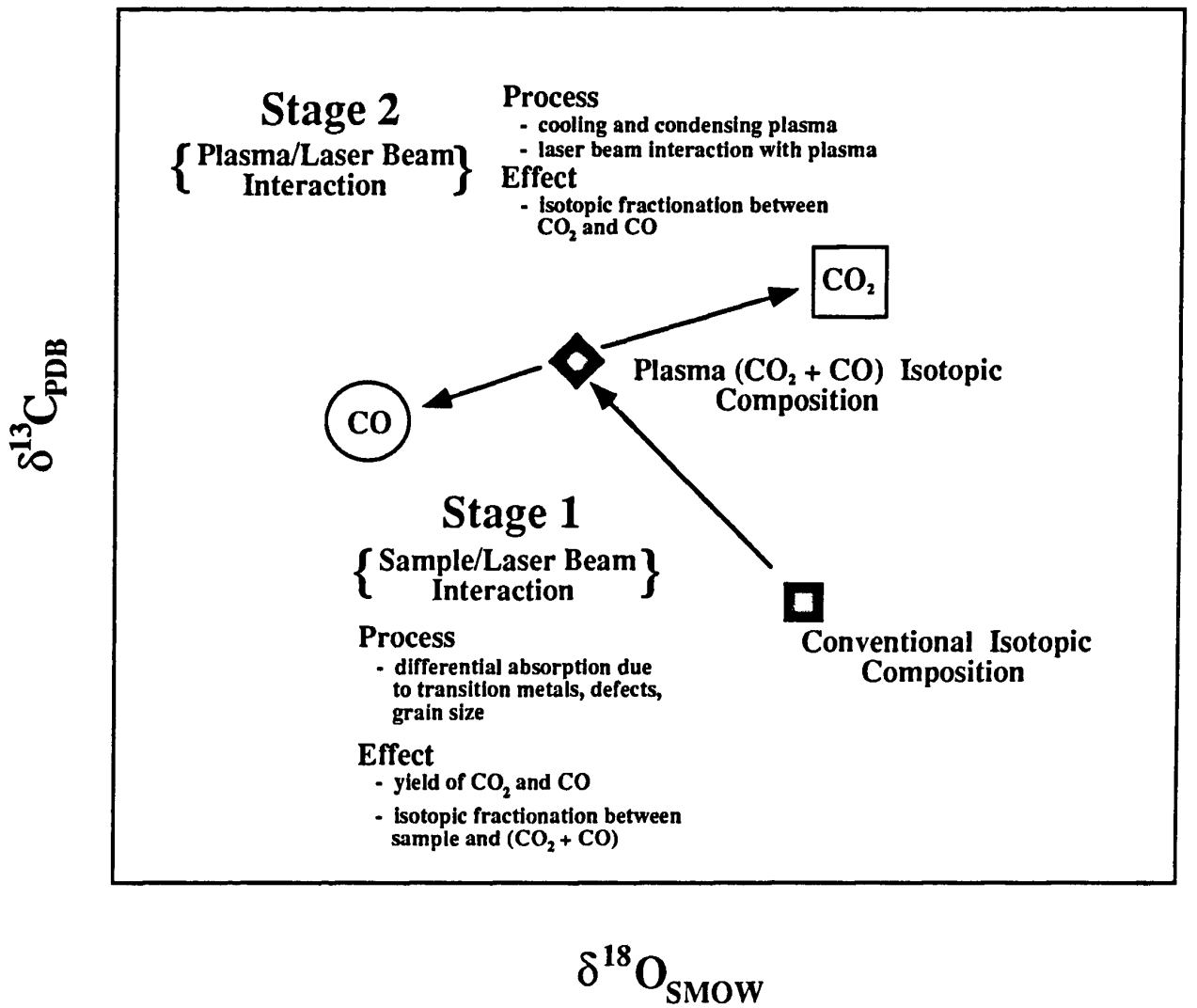


Figure 12. A two-stage model describing the processes occurring during laser ionization of carbonate minerals and the resulting effects on the isotopic compositions of product gases. Stage 1 is controlled mainly by the absorption characteristics of the sample and affects the yields and ratios of $CO_2$ and CO, and also the isotopic composition of combined $CO_2$ and CO. Stage 2 is controlled by the cooling and condensing plasma, including interactions between the plasma cloud and the laser beam. Stage 2 primarily effects the isotopic fractionation between $CO_2$ and CO.

with the Nd:YAG laser (Fig. 12). Stage one commences when the laser beam initially excites the sample surface and encompasses all interactions between the laser beam and the mineral. The absorption characteristics of the mineral encountered in stage one ultimately influence the $\delta^{13}C$ and $\delta^{18}O$ values of the ionized plume, the yield of gas per laser pulse, and the $CO_2/CO$ ratio. Stage two begins with the formation of an ion/gas plume and involves all interaction between laser photons and the expanding plume, and reactions within the cooling plume. When the plume has formed stable chemical phases, including CO and $CO_2$, stage two is complete. During stage two, CO and $CO_2$ are isotopically fractionated from one another by approximately 0.5°/oo to 2°/oo in carbon and 2°/oo to 5°/oo in oxygen, with $CO_2$ being enriched in both $^{13}C$ and $^{18}O$ relative to CO (Fig. 9) as determined by experiments discussed earlier.

### 3.2.2 Absorption Effects

The absorption characteristics of a mineral are controlled mainly by its chemical composition, but are also influenced by factors such as grain size and presence of crystal defects. When a laser photon interacts with a mineral surface it can be reflected, refracted, or absorbed. If the probability of absorption is high, the sample can be easily ionized by the laser beam and converted to gas. One method of increasing absorption is to powder the sample, as did Smalley

and his associates, which increases photon interactions with mineral surfaces, thereby increasing the number of absorptions. To assess this effect in the system at the University of Saskatchewan, calcite sample MM was analyzed as a finely powdered pellet (MMP) (Table 4). The results show increased CO and $CO_2$ yields per pulse, increased $CO_2$/CO ratios, and different isotopic compositions of both CO and $CO_2$ relative to previous in situ laser analysis (Fig. 13). Although this approach increases the yield, $\delta^{13}C$ and $\delta^{18}O$ values remain different from conventional analyses. Isotope correction factors based on results from powdered samples may not be applicable to in situ results. Most importantly though, powdering the samples defeats the purpose of in situ analysis.

Infrared spectra of calcite, dolomite, rhodochrosite, and siderite were examined near the region of the Nd:YAG laser wavelength (Fig. 14) to determine the absorption characteristics of each carbonate. Calcite and dolomite have relatively high reflectivities in the region of 1.0$\mu$m, whereas siderite and rhodochrosite have broad absorption peaks from 1.0$\mu$m to 1.5$\mu$m. Hunt and Salisbury (1971) proposed that the increased absorption of siderite and rhodochrosite is due to the presence of $Fe^{2+}$ in the specimens they measured. When $Fe^{2+}$ is bonded in an octahedral field the d-orbitals split into two sets of degenerate orbitals consisting of one set of low energy bonding orbitals and one set of higher energy non-

TABLE 4

Laser-Assisted Analyses of Powdered Carbonate.

| Sample No. | L. E., Mode, Style | $\delta^{18}O_{SMOW}$ | $\delta^{13}C_{PDB}$ |
|---|---|---|---|
| MM-0-#3(Std) | n.a. | 28.86 | 2.11 |
| MM-0-#4(Std) | n.a. | 28.82 | 2.11 |
| MM-0-#2(Std) | n.a. | 28.82 | 2.09 |
| MM-0-#1(Std) | n.a. | 28.87 | 2.11 |
| MM-0-#5(Std) | n.a. | 28.77 | 2.05 |
| MMP-8a(Comb) | 60, L.P., Grid | 23.7 | 3.6 |
| MMP-9a(Comb) | 60, L.P., Grid | 28.8 | 4.9 |
| MMP-10(Comb) | 65, L.P., Grid | 30.8 | 4.9 |
| MMP-11(Comb) | 65, L.P., Grid | 30.7 | 4.6 |
| MMP-12(Comb) | 70, L.P., Grid | 30.5 | 4.6 |
| MMP-13(Comb) | 70, L.P., Grid | 30.7 | 4.5 |
| MMP-14(CO) | 65, L.P., Grid | 30.3 | 3.9 |
| MMP-14(CO2) | | 31.9 | 4.6 |
| MMP-15(CO) | 65, L.P., Grid | 29.5 | 3.8 |
| MMP-15(CO2) | | 33.4 | 4.9 |

MMP=powdered calcite;(Std)=isotopic composition determined by acid dissolution; (Comb)=isotopic compositions of CO and $CO_2$ determined together; (CO)=isotopic composition of CO only; ($CO_2$)= isotopic composition of $CO_2$ only; L.E.= lamp energy; Mode= laser operating mode; Style= ionization technique; L. P.=long pulse; Grid= multi-point ionization style; unless otherwise specified, samples were analyzed using the Nd:YAG laser; n.a.= not applicable.

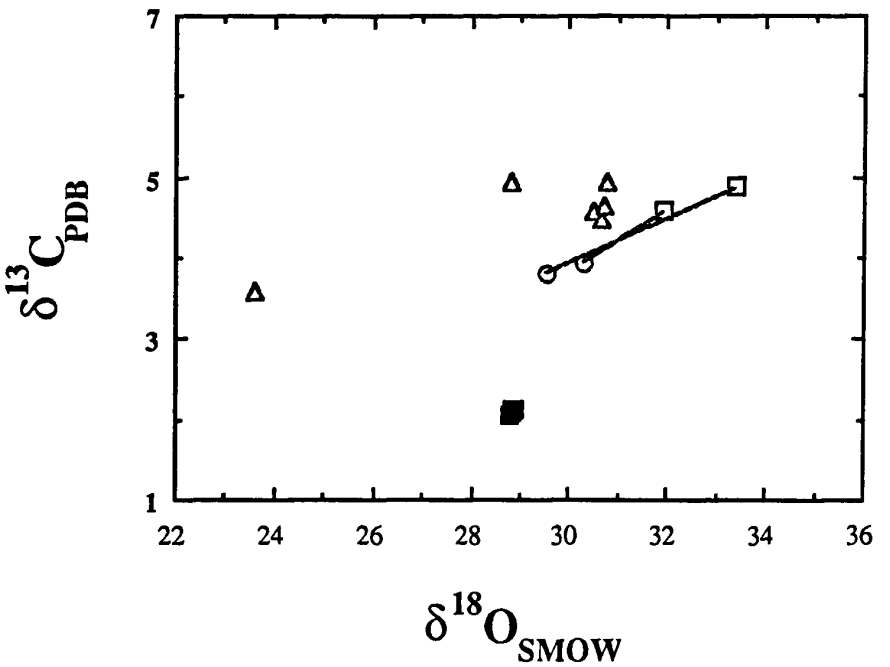


**Figure 13. Isotopic compositions of CO (○) $CO_2$(□) and combined gases (Δ) produced during laser ionization of the powdered calcite (MMP). Compared to the unpowdered results in Figure 9 and 10 for calcite (MM), the isotopic compositions of the gases are different. Note that $CO_2$ is enriched in $^{13}C$ and $^{18}O$ relative to CO as indicated by the tie-lines which connect gases formed during the same experiment. The isotopic compositions of the carbonates determined by acid dissolution are also shown (▩).**

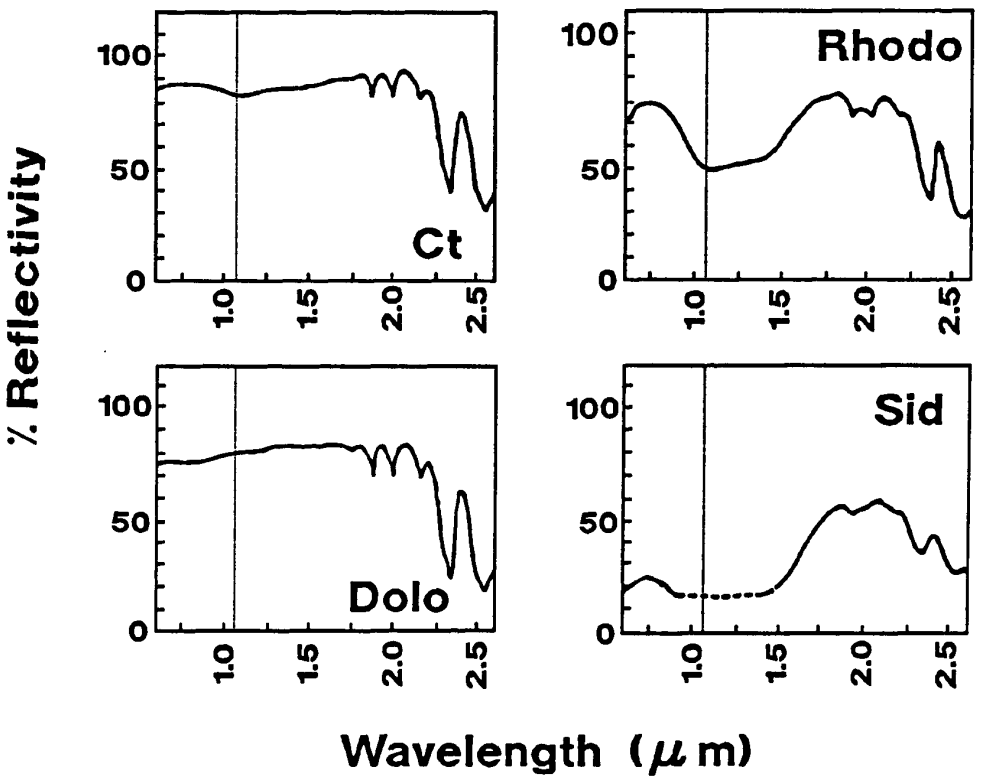


Figure 14. Infrared spectra of calcite, dolomite, rhodochrosite, and siderite in the region of the Nd:YAG laser wavelength (dotted lines at 1.064 μm) showing the effect of Fe on the absorption characteristics of carbonate minerals (after Hunt and Salisbury, 1971).

bonding orbitals. Absorption of photons with wavelengths between 1.0$\mu$m and 1.5$\mu$m are thought to be related to electronic transitions between these two sets of d-orbitals. Many carbonate spectra measured by Hunt and Salisbury (1971) including azurite, malachite, and smithsonite, all containing transition metal cations, show significant absorption in the region of 1.0$\mu$m even when iron is present only in trace amounts. This may indicate that absorption of Nd:YAG radiation is enhanced not only by iron, but by other transition metals as well, in carbonate phases.

In trigonal carbonate minerals the metal cations are positioned in atomic layers that alternate with layers of $CO_3^{2-}$ anions. If the probability of absorption is relatively low, as in the case of calcite and dolomite, photon absorption will disrupt the crystal structure and produce a plume of particles ranging in size from cleavage fragments to ions. As the cloud cools, some ions will form stable gases like CO and $CO_2$. If the probability of absorption is high because of the presence of transition metal cations in the mineral, such as for rhodochrosite and siderite, the absorption of photons occurs preferentially in the metal cation layers and produces a plume of particles also ranging in size, but relatively enriched in ions. It is through this type of process that the efficiency of the laser beam yields a quantity of gas for every pulse. The $CO_2$/CO ratios also are correlative with photon absorption, however, the exact process controlling the ratios is

uncertain. However, if transition metal-oxygen bonds are preferentially broken the formation of $CO_3$ ions is favoured producing a plume enriched in $CO_2$, if the metal-oxygen bond is not preferentially broken the crystal structure is disrupted in a random fashion, especially on crystal defects, producing a plume relatively enriched in CO. This is indirectly supported by the $CO_2$ laser results. The $CO_2$ laser energy is absorbed by C-O bonds, and CO is essentially the only gas produced by laser ionization, independent of transition metal content.

As the plasma cloud cools it forms stable gases of which CO and $CO_2$ represent the majority of the gaseous carbon and oxygen bearing phases. The $\delta^{13}C$ and $\delta^{18}O$ values of the combined CO and $CO_2$ (Fig. 10) are not equivalent to those of the sample, implying that some carbon and oxygen must be retained either in the sample chamber or in the sample. Incomplete ionization during absorption of the laser energy by the sample, or the formation of stable residual products containing carbon and oxygen which condense and fall out of the ion plume are most likely responsible for the significant differences between the $\delta^{13}C$ and $\delta^{18}O$ values of combined CO and $CO_2$ relative to the actual isotopic composition of the sample. These processes are probably affected by chemical composition because $\delta^{13}C$ and $\delta^{18}O$ values of combined CO and $CO_2$ are not consistently fractionated from the mineral isotopic

composition for different carbonate minerals.

Stage two represents the transformation of the ionized gas plume to stable gases and includes the interaction between an incoming laser beam and the ion plume. Although individual pulse-widths are only 8ns to 9ns long, the total pulse consists of 50 to 100 individual pulses separated by 2$\mu$s to 4$\mu$s making the total pulse-width approximately 200$\mu$s. This leaves ample time for the latter part of the pulse to interact with the expanding ion plume produced by the initial part of the pulse. As the plasma cloud cools, CO and $CO_2$ are formed with similar relative isotopic fractionations between them, a process which is independent of the carbonate mineral being analyzed (Fig. 9). $CO_2$ is enriched in $^{13}C$ and $^{18}O$ relative to CO, in marked contrast to equilibrium fractionations that predict $CO_2$ should be enriched in $^{13}C$ but depleted in $^{18}O$ relative to CO (Richet et al., 1977). This implies that processes in the cooling ion plume are kinetically controlled and that significant, non-equilibrium fractionations occur in the laser ionization process despite the extremely high energies and temperatures involved.

Kelley and Fallick (1990) and Crowe et al. (1990) have successfully measured $\delta^{34}S$ values in sulphide minerals using a Nd:YAG laser extraction system. Sulphides have very high photon absorption because of their high concentrations of transition metal cations. The small correction factors determined by these workers suggest that sulphur from the

mineral is almost completely converted to $SO_2$, and that problems of incomplete ionization, formation of residual compounds, and kinetic interferences occur but are less substantial than with carbonate minerals.

# 4. RESULTS AND DISCUSSION OF HYDROUS MINERAL ANALYSES

## 4.1 Results from Laser-Assisted Analyses of the Hydrous Mineral Samples

The first $\delta D$ analyses using laser ionization were done without exposure of gases released to CuO at 550°C before cryogenically trapping the gases at -196°C, a routine procedure in the conventional method (e.g. Kyser and O'Neil, 1984). The initial $\delta D$ values determined for biotite sample PBT, without exposure to CuO, were close to the value of $-99^{\circ}/_{oo}$ measured conventionally, but lacked precision (Table 5). The function of the CuO is to oxidize hydrogenic gas species such as $H_2$, HCl, and HF to $H_2O$. Subsequent analyses included exposure of the gases to hot CuO which resulted in $\delta D$ values more depleted than the values determined without CuO, but with increased precision and yield (Table 5). A comparison of results with and without CuO demonstrates that a significant portion of the hydrogen released from laser ionization of hydrous minerals is not in the form of $H_2O$.

### 4.1.1 Geological, Chemical, and Isotopic Data of the Hydrous Mineral Samples

Hydrous minerals used to test the laser ionization system consisted of three different micas, two amphiboles, and two evaporite minerals. All samples were tested to ensure both their chemical (Table 6) and isotopic homogeneity (Tables 5 and 7). Chemical homogeneity was determined by major element

Table 5.

Laser Ionization Data of Micas, Amphiboles, and Kaolinite

| Sample No. | L.E., Mode, Style | Time (mins) | Weight % $H_2O$ | Pulses | µmoles $H_2O$ (yield) | $\delta D_{Laser}$ | $\delta D_{Corr}$ |
|---|---|---|---|---|---|---|---|
| K21-0(Std) | n.a. | n.a. | 10.70 | n.a. | n.a. | n.a. | -42 |
| K21-1 | 60, Qsw, S.P. | 0 | 10.70 | 300 | 2.76 | -179 | -194 |
| K21-2 | 60, Qsw, S.P. | 42 | 10.70 | 300 | 1.84 | -179 | -194 |
| K21-3 | 60, Qsw, S.P. | 112 | 10.70 | 450 | 2.07 | -169 | -183 |
| K21-4 | 60, Qsw, S.P. | 168 | 10.70 | 500 | 2.17 | -152 | -165 |
| MAR-26-0(Std) | n.a. | n.a. | 3.23 | n.a. | n.a. | n.a. | -62 |
| MAR-26-1 | 60-Qsw/60-LP,S.P. | 0 | 3.23 | 250/100 | 2.33 | -177 | -192 |
| MAR-26-2 | 60-Qsw/60-LP,S.P. | 43 | 3.23 | 300/120 | 1.81 | -178 | -193 |
| MAR-26-3 | 60, Qsw, S.P. | 377 | 3.23 | 250 | 1.12 | -159 | -173 |
| RHM-411-0(Std) | n.a. | n.a. | 4.10 | n.a. | n.a. | n.a. | -63 |
| RHM-411-1 | 60-Qsw/60-LP,S.P. | 0 | 4.10 | 220/50 | 4.73 | -164 | -178 |
| RHM-411-2 | 60-Qsw/60-LP,S.P. | 58 | 4.10 | 200/100 | 2.42 | -165 | -179 |
| RHM-411-3 | 60-Qsw/60-LP,S.P. | 102 | 4.10 | 200/100 | 2.38 | -157 | -171 |
| RHM-411-4 | 60, Qsw, S.P. | 0 | 4.10 | 100 | 3.03 | -169 | -183 |
| RHM-411-5 | 60, Qsw, S.P. | 49 | 4.10 | 100 | 1.58 | -152 | -165 |
| RHM-411-6 | 60, Qsw, S.P. | 86 | 4.10 | 100 | 1.52 | -138 | -150 |
| RHM-411-7 | 60, Qsw, S.P. | 1239 | 4.10 | 100 | 1.13 | -154 | -167 |
| PMS-0(Std) | n.a. | n.a. | 3.55 | n.a. | n.a. | n.a. | -65 |
| PMS-10 | 65, LP, grid | n.a. | 3.55 | n.d. | 9.40 | -116 | -133 |
| PMS-11 | 65, LP, grid | n.a. | 3.55 | n.d. | 9.12 | -116 | -133 |
| RHM-409P-0(Std) | n.a. | n.a. | 3.10 | n.a. | n.a. | n.a. | -68 |
| RHM-409P-5 | 60-Qsw/60-LP,S.P. | 60 | 3.10 | 200/150 | 1.29 | -176 | -191 |
| RHM-409P-6 | 60-Qsw/60-LP,S.P. | 108 | 3.10 | 200/150 | 2.30 | -185 | -200 |
| RHM-409P-7 | 60-Qsw/60-LP,S.P. | 445 | 3.10 | 260/200 | 1.50 | -179 | -194 |
| RHM-409P-8 | 60-Qsw/60-LP,S.P. | 488 | 3.10 | 250/150 | 1.25 | -163 | -177 |
| RHM-409P-9 | 60-Qsw/60-LP,S.P. | 0 | 3.10 | 250/150 | 1.79 | -180 | -195 |
| RHM-409P-10 | 60-Qsw/60-LP,S.P. | 154 | 3.10 | 300/150 | 1.35 | -149 | -162 |
| RHM-409P-11 | 60-Qsw/60-LP,S.P. | 517 | 3.10 | 250/150 | 1.74 | -185 | -200 |
| HBL-14-0(Std) | n.a. | n.a. | 2.40 | n.a. | n.a. | n.a. | -79 |
| HBL-14-11 | 60-Qsw/40-LP, S.P. | 0 | 2.40 | 200/100 | 2.06 | -173 | -188 |
| HBL-14-12 | 60-Qsw/40-LP, S.P. | 46 | 2.40 | 250/150 | 2.03 | -173 | -188 |
| HBL-14-13 | 60-Qsw/40-LP, S.P. | 87 | 2.40 | 250/100 | 1.61 | -168 | -182 |
| HBL-14-15 | 60-Qsw/40-LP, S.P. | 825 | 2.40 | 200/100 | 1.14 | -180 | -195 |
| PBT-0(Std) | n.a. | n.a. | 1.60 | n.a. | n.a. | n.a. | -99 |
| PBT-2 | 60, LP, grid | n.d. | 1.60 | n.d. | n.d. | -85 | -94 |
| PBT-4 | 60. LP, grid | n.d. | 1.60 | n.d. | n.d. | -107 | -117 |
| PBT-5 | 60, LP, grid | n.d. | 1.60 | n.d. | n.d. | -117 | -128 |
| PBT-9 | 60, LP, grid | n.d. | 1.60 | 230 | 3.08 | -145 | -158 |
| PBT-10 | 70, LP, grid | n.d. | 1.60 | 400 | 3.06 | -149 | -162 |
| PBT-11 | 60, LP, grid | n.d. | 1.60 | 195 | 1.95 | -140 | -152 |
| PBT-20 | 60-Qsw/40-LP, S.P. | n.d. | 1.60 | 200/100 | n.d. | -160 | -174 |
| PBT-21 | 60-Qsw/40-LP, S.P. | n.d. | 1.60 | 350/100 | 1.29 | -164 | -178 |
| PBT-23 | 60, Qsw, S.P. | n.d. | 1.60 | 300 | 0.02 | -187 | -203 |
| RHM-409A-0(Std) | n.a. | n.a. | 1.71 | n.a. | n.a. | n.a. | -103 |
| RHM-409A-1 | 60-Qsw/40-LP, S.P. | 0 | 1.71 | 200/100 | 3.93 | -180 | -195 |
| RHM-409A-2 | 60-Qsw/50-LP, S.P. | 45 | 1.71 | 250/100 | 2.03 | -164 | -178 |
| RHM-409A-3 | 60-Qsw/60-LP,S.P. | 87 | 1.71 | 250/100 | 1.94 | -176 | -191 |
| RHM-409A-4 | 60-Qsw/60-LP,S.P. | 0 | 1.71 | 260/200 | 1.27 | -179 | -194 |
| D46G2-0(Std) | n.a. | n.a. | 2.82 | n.a. | n.a. | n.a. | -104 |
| D46G2-1 | 60-Qsw/60-LP,S.P. | 0 | 2.82 | 200/100 | 1.76 | -205 | -222 |
| D46G2-2 | 60-Qsw/60-LP,S.P. | 958 | 2.82 | 250/100 | 1.55 | -192 | -208 |
| D46G2-3 | 60, Qsw, S.P. | 1018 | 2.82 | 400 | 1.27 | -187 | -203 |
| D46G2-4 | 60, Qsw, S.P. | 0 | 2.82 | 350 | 1.52 | -179 | -194 |
| D46G2-5 | 60, Qsw, S.P. | 65 | 2.82 | 400 | 1.28 | -206 | -223 |
| D46G2-6 | 60, Qsw, S.P. | 344 | 2.82 | 600 | 1.48 | -210 | -227 |
| D46G2-7 | 60, Qsw, S.P. | 0 | 2.82 | 300 | 1.65 | -210 | -227 |
| D46G2-9 | 60-Qsw/60-LP, S.P. | 345 | 2.82 | 400/100 | 1.40 | -211 | -228 |
| D46G2-10 | 60, Qsw, S.P. | 1392 | 2.82 | 500 | 1.23 | -225 | -243 |
| D46G2-12 | 60-Qsw/60-LP, S.P. | 1502 | 2.82 | 500/100 | 1.20 | -200 | -216 |
| D46G2-13 | 60-Qsw/60-LP, S.P. | 2831 | 2.82 | 500/100 | 1.39 | -212 | -229 |
| D46G2-14 | 60, Qsw, S.P. | 2893 | 2.82 | 600 | 1.01 | -186 | -200 |

K21= kaolinite sample; MAR-26, RHM-411, RHM-409P = phlogopite samples; PMS= muscovite sample; PBT= biotite sample; HBL-14,RHM-409A, D46G2= amphibole samples; L.E.= lamp energy; Qsw= Q - switched mode; L.P.= long pulse mode; Style= ionization style; Time= time in mins between loading and analysis; S.P.= single pit; grid= closely spaced pits; Pulses= total pulses Qsw/L.P. impinged onto the sample ; $\delta D_{Laser}$=raw laser values; $\delta D_{Corr}$=corrected laser values; n.a.= not applicable; (Std)=isotopic composition determined by conventional technique.

## TABLE 6

Microprobe Data for H-bearing Minerals

| Sample No. | K-21 | MAR-26 | RHM-411 | RHM-409 | HBL-14 | RHM-409 | D46G2 |
|---|---|---|---|---|---|---|---|
| Mineral | Kaolinite | Phlogopite | Phlogopite | Phlogopite | Amphibole | Amphibole | Amphibole |
| SiO2 | 48.33 | 41.65 | 41.82 | 42.35 | 44.86 | 53.83 | 41.06 |
| TiO2 | 0.00 | 1.08 | 0.57 | 2.10 | 0.71 | 0.66 | 0.52 |
| Al2O3 | 38.74 | 9.86 | 10.52 | 9.46 | 10.04 | 1.05 | 9.90 |
| Cr2O3 | 0.00 | 0.17 | 0.23 | 0.16 | 0.00 | 0.11 | 0.00 |
| FeO | 0.46 | 6.73 | 4.19 | 6.75 | 15.39 | 3.92 | 23.53 |
| MnO | 0.00 | 0.06 | 0.02 | 0.03 | 0.22 | 0.05 | 1.65 |
| MgO | 0.06 | 24.26 | 25.57 | 22.89 | 12.22 | 21.04 | 6.55 |
| CaO | 0.06 | 0.00 | 0.01 | 0.06 | 10.63 | 6.98 | 10.36 |
| NiO | 0.00 | 0.09 | 0.15 | 0.13 | 0.05 | 0.03 | 0.06 |
| Na2O | 0.06 | 0.13 | 0.20 | 0.05 | 1.71 | 3.12 | 1.92 |
| K2O | 0.10 | 10.26 | 10.40 | 9.97 | 0.27 | 5.18 | 1.52 |
| F | n.d. | 0.32 | 0.38 | 0.29 | 0.00 | 0.36 | 0.89 |
| Cl | n.d. | 0.04 | 0.05 | 0.01 | 0.20 | 0.01 | 0.07 |
| H2O(Iso) | 10.70 | 3.23 | 4.10 | 3.10 | 2.40 | 1.71 | 2.82 |
| Total | 98.51 | 97.90 | 98.21 | 97.36 | 98.68 | 98.05 | 100.88 |
| | | | | | | | |
| Si | 4.317 | 6.153 | 6.036 | 6.276 | 6.678 | 7.812 | 6.314 |
| Al | - | 1.715 | 1.788 | 1.651 | 1.322 | 0.179 | 1.686 |
| | | | | | | | |
| Al | 4.075 | 0.000 | 0.000 | 0.000 | 0.438 | 0.000 | 0.107 |
| Ti | 0.000 | 0.120 | 0.619 | 0.234 | 0.079 | 0.720 | 0.060 |
| Fe | 0.034 | 0.832 | 0.506 | 0.837 | 1.916 | 0.476 | 3.026 |
| Mn | 0.000 | 0.008 | 0.002 | 0.004 | 2.711 | 0.006 | 0.215 |
| Mg | 0.008 | 5.342 | 5.501 | 5.056 | 0.028 | 4.550 | 1.501 |
| Ni | 0.000 | 0.020 | 0.017 | 0.015 | 0.006 | 0.004 | 0.007 |
| Cr | 0.000 | 0.011 | 0.026 | 0.019 | 0.000 | 0.012 | 0.000 |
| | | | | | | | |
| Ca | 0.006 | 0.000 | 0.002 | 0.010 | 1.696 | 1.085 | 1.707 |
| Na | 0.010 | 0.037 | 0.055 | 0.014 | 0.486 | 0.865 | 0.564 |
| K | 0.011 | 1.934 | 1.915 | 1.885 | 0.513 | 0.959 | 0.298 |
| | | | | | | | |
| OH | 6.375 | 3.183 | 3.947 | 3.064 | 2.383 | 1.655 | 2.892 |
| F | n.d. | 0.149 | 0.173 | 0.136 | 0.000 | 0.165 | 0.433 |
| Cl | n.d. | 0.010 | 0.012 | 0.003 | 0.050 | 0.002 | 0.018 |

Table 7.

Laser-Assisted Analyses of Carnallite and Fluid Inclusions in Halite.

| Sample No. | L.E., Mode | Weight (mg). | Weight % $H_2O$ | Weight % $H_2O$ (calc) | µmoles $H_2O$ (yield) | $\delta D_{Laser}$ | $\delta D_{Corr}$ |
|---|---|---|---|---|---|---|---|
| BE503-0(Std) | n.a. | n.a. | 37.00 | n.a. | n.a. | n.a. | -70 |
| BE503-1 | 40, Qsw | 38.81 | - | 0.28 | 6.02 | -133 | -151 |
| BE503-2 | 40, Qsw | 40.02 | - | 0.38 | 8.55 | -142 | -161 |
| BE503-3 | 40, Qsw | 72.51 | - | 0.15 | 6.23 | -118 | -135 |
| BE503-4 | 40, Qsw | 28.51 | - | 0.63 | 9.95 | -116 | -133 |
| BE503-5 | 40, Qsw | 34.49 | - | 0.61 | 11.74 | -131 | -149 |
| LPE2-0(Std) | n.a. | n.a. | 37.00 | n.a. | n.a. | n.a. | -126 |
| LPE2-1 | 30, Qsw | 5.00 | - | 0.92 | 2.56 | -129 | -140 |
| LPE2-2 | 40, Qsw | 9.90 | - | 0.41 | 2.23 | -126 | -138 |
| LPE2-3 | 40, Qsw | 31.32 | - | 0.29 | 4.97 | -142 | -161 |
| LPE2-4 | 40, Qsw | 39.62 | - | 0.36 | 7.92 | -157 | -178 |
| LPE2-5 | 40, Qsw | 32.06 | - | 0.49 | 8.73 | -140 | -159 |
| SYN-D-0(Std) | n.a. | n.a. | 2.20 | n.a. | n.a. | n.a. | -17 |
| SYN-D-1 | 30, Qsw | 16.46 | - | 0.52 | 4.73 | -126 | -138 |
| SYN-D-2 | 30, Qsw | 22.61 | - | 0.12 | 1.48 | -69 | -77 |
| SYN-D-3 | 30, Qsw | 14.09 | - | 0.53 | 4.12 | -110 | -121 |
| SYN-D-4 | 30, Qsw | 21.58 | - | 0.48 | 5.75 | -131 | -143 |
| SYN-D-5 | 30, Qsw | 15.18 | - | 0.34 | 2.87 | -119 | -130 |
| SYN-B-0(Std) | n.a. | n.a. | 2.20 | n.a. | n.a. | n.a. | -136 |
| SYN-B-1 | 30, Qsw | 8.70 | - | 0.53 | 2.56 | -154 | -167 |
| SYN-B-2 | 30, Qsw | 8.90 | - | 0.30 | 1.50 | -145 | -158 |
| SYN-B-3 | 30, Qsw | 10.00 | - | 0.33 | 1.85 | -122 | -133 |
| SYN-B-4 | 30, Qsw | 7.22 | - | 0.52 | 2.08 | -150 | -163 |
| SYN-B-5 | 30, Qsw | 14.84 | - | 0.69 | 5.67 | -167 | -181 |

BE503 and LPE2 are natural carnallite samples; SYN-B and SYN-D are synthetic halite samples; (Std)= isotopic composition determined by conventional technique; L.E.= lamp energy; Mode= laser operating mode; Qsw= Q-switched mode; sample weights are in milligrams; $\delta D_{Laser}$= raw laser values; $\delta D_{Corr}$= corrected laser values using Fig. 3; n.a.= not applicable.

analysis using an electron microprobe and the data reported in Table 6 is derived from at least three analyses. Isotopic homogeneity was verified by at least two but more commonly three analyses of each sample, where the sample material was taken from separate regions of larger samples when possible.

The single mineral hydrous silicates samples are biotite (PBT), muscovite (PMS), and kaolinite (K21). These first two samples were chosen because they are physically large specimens of a single mineral. Muscovite (PMS) and biotite (PBT) samples were taken from large (4X5cm) crystals formed in a pegmatitic environment. The biotite sample is from Sebastapol, Ontario, and the muscovite sample is from Pied des Mont, Quebec. These samples can be mounted in the sample chamber with only minor sample preparation. A pure kaolinite sample (K21 and K21X), which is a pure mineral separate from a formation in the Athabasca Basin in northern Saskatchewan, was powdered and pressed into two small pellets (2 cm dia.). One pellet was used for routine laser analysis and the other for an absorbtion experiment discussed later.

Rock thick-sections analyzed consist of three MARID (mica, amph., rutile, ilmenite, and diopside) xenoliths MAR-26 and RHM-409 composed primarily of phlogopite, diopsidic clinopyroxene, and K-richterite amphibole, and RHM-411 a phlogopite-amphibole-bearing partially serpentinized sample. The MARID samples were collected from the Bultfontein kimberlite in Kimberly, South Africa. Sample MAR-26 is well

foliated with a ground mass of mainly phlogopite, with approximately 5% carbonate and 5% clay minerals. The phenocrysts consist of 60% phlogopite, 15% diopside, and 15% K-richterite with minor ilmenite. Laser sampling was performed on the phenocrystic phlogopite. Sample RHM-409 is similar to MAR-26 except that phologopite makes up approximately 85% of the thin section, including all of the groundmass. Laser sampling was performed on the phenocrysts of phlogopite and richterite. Sample RHM-411 is also a MARID xenolith even though it contains olivine. The rock consists of 50% serpentinized olivine, 25% phlogopite, 10% diopside, 10% amphibole, with minor opaque minerals. The phlogopite was sampled with the laser system.

Two large hornblende crystals (D46G2 and HBL-14) that contain some minor impurities were sampled using the laser system. Both samples are 95% hornblende, HBL-14 also contains approximately 2% biotite and 1% opaque minerals, and D46G2 also contains 2% quartz, 2% chlorite and muscovite, and 1% opaque minerals. These hornblende samples were obtained from the Department of Geological Sciences mineral collection at the University of Saskatchewan.

Two samples of natural carnallite (BE503 and LPE2) and two samples of synthetically produced fluid inclusion-rich halite (SYN-B and SYN-D) were also studied. The carnallite samples were collected from a potash mine in Saskatchewan. The synthetic halite samples were precipitated from halite

saturated aqueous solutions of known hydrogen isotopic compositions in the laboratory. SYN-B halite was precipitated form a solution with $\delta D=-136^{\circ}/_{oo}$ and SYN-D was precipitated from a solution with $\delta D=-17^{\circ}/_{oo}$.

### 4.1.2 Results from Laser-Assisted Analyses of Hydrous Silicate Samples

With only one exception, all the $\delta D$ values ($\delta D_{corr}$), corrected using the isotope calibration curve (Fig. 3), are depleted in D relative to the values determined using the conventional technique. In addition, similar types of minerals do not have the same fractionations relative to conventional $\delta D$ values, even from two samples of amphibole (D46G2 and RHM-409A) that have identical $\delta D$ values.

Calculation of the expected yield of water from a hydrous silicate sample can be obtained by estimating the volume of material ionized by the laser beam and using the wt%$H_2O$ of the sample determined with the conventional method and the density of the mineral. One must assume all of the water is recovered from the ionized material. For example, phlogopite RHM-411 with 4.1wt%$H_2O$ and a density of 3.1g/cm$^3$ should yield approximately 7$\mu$moles of $H_2O$ from ionization of a 1mm by 1mm by 1mm volume of sample, and a 500$\mu$m by 500$\mu$m by 500$\mu$m volume should yield 0.4$\mu$moles of $H_2O$.

It is difficult to accurately estimate the volume of material removed from a laser ionization pit, especially when

the percentage of unionized material ejected from the pit is not known. However, it is safe to assume that an average volume of material removed from the each sample for all the hydrous silicate analyses is greater than or equal to $1mm^3$. Thus the expected yield of $H_2O$ from relatively water-poor samples such as RHM-409A and PBT should be a minimum of 3$\mu$moles of $H_2O$. The average yield of $H_2O$ for all of the hydrous silicate analyses is 1.87$\mu$moles ranging from 1$\mu$mole to 5$\mu$moles (Table 5). This implies that the ionization process is not efficiently sampling water from the ionized material.

Analysis PBT-23 of the biotite sample was a test for potential surface contamination. Prior to collecting a water sample for analysis a relatively large area ($2mm^2$) of the sample surface was rastered away with the laser in Q-Switched mode to a depth of approximately 500$\mu$m. Then analysis of the presumably pristine material now exposed was performed using the same method used for previous analyses of the biotite sample. The $\delta D$ value determined for the "non-surficial" biotite was similar to previous results obtained using laser ionization. This suggests that, if contamination of the samples by surface absorbed water occurs, it is pervasive on the scale of millimeters.

### 4.1.3 Time Dependent Yield and Isotopic Shifts

Subsequent analyses using laser-assisted extraction of the same hydrous mineral produced results that changed

consistently relative to the previous analysis. Most notably, the yield of hydrogen per laser pulse impinged onto the sample decreased (Fig. 15) and the $\delta D$ value of that hydrogen normally increased (Fig. 16). The elapsed time is the time interval between the first analysis and each subsequent analysis without exposure of the sample to atmosphere in between analyses. As the elapsed time increases, the relative yield of water decreases (Fig. 15).

In many cases the yield of water from subsequent analyses continued to decrease despite having to impinge a greater number of laser pulses onto the sample to obtain enough water for an accurate analysis. Only a portion of the data in Table 5 is plotted on Figure 15 to demonstrate this trend, however, most of the groups of analyses show a loss of yield per pulse through time.

Concurrent with a decreases in yield, the $\delta D$ values of the hydrogen released by laser ionization also increase toward the conventionally determined isotopic value as elapsed time increases (Fig. 16). The most probable explanation of the decrease in yield per pulse and increase in $\delta D$ is that hydrogen with a low $\delta D$ value is being removed from the samples by the vacuum.

### 4.1.4 Results from Laser-Assisted Analyses of the Evaporite Mineral Samples

The procedure used for laser-based analyses of evaporite

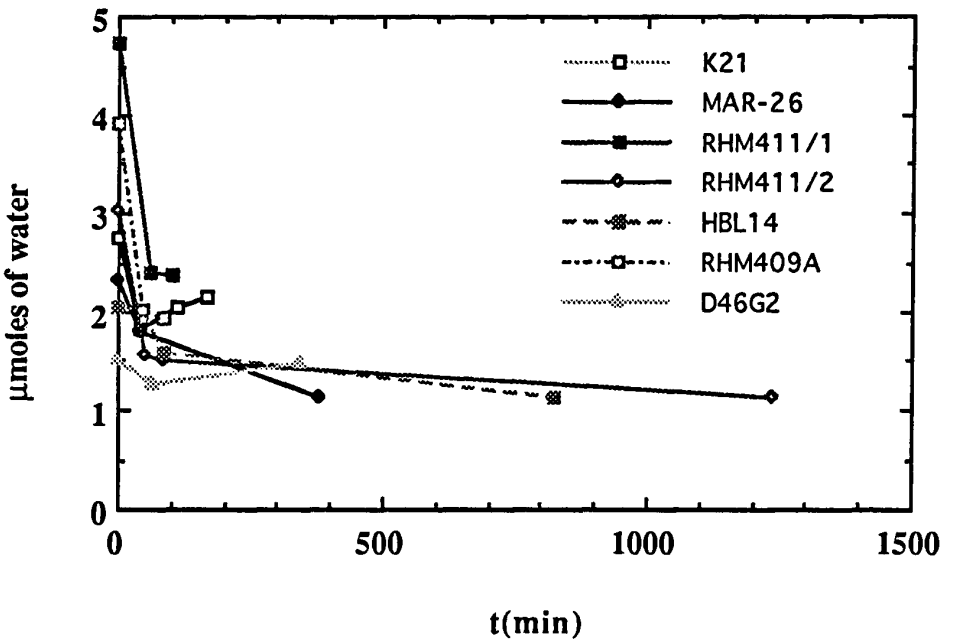


Figure 15. Relationship between the yield of water (µmoles) released from various hydrous minerals using the Nd:YAG laser and the time (min) the samples were under vacuum in the sample chamber prior to analysis is shown. All samples show a marked early decrease in the amount of water released during the first hour in vacuum and many of the samples show continued decrease in yield of water for analyses up to 20 hours later. Some samples show increased yields after the first hour, but this because a greater number of laser pulses were impinged onto the sample to provide a large enough sample for accurate analysis.

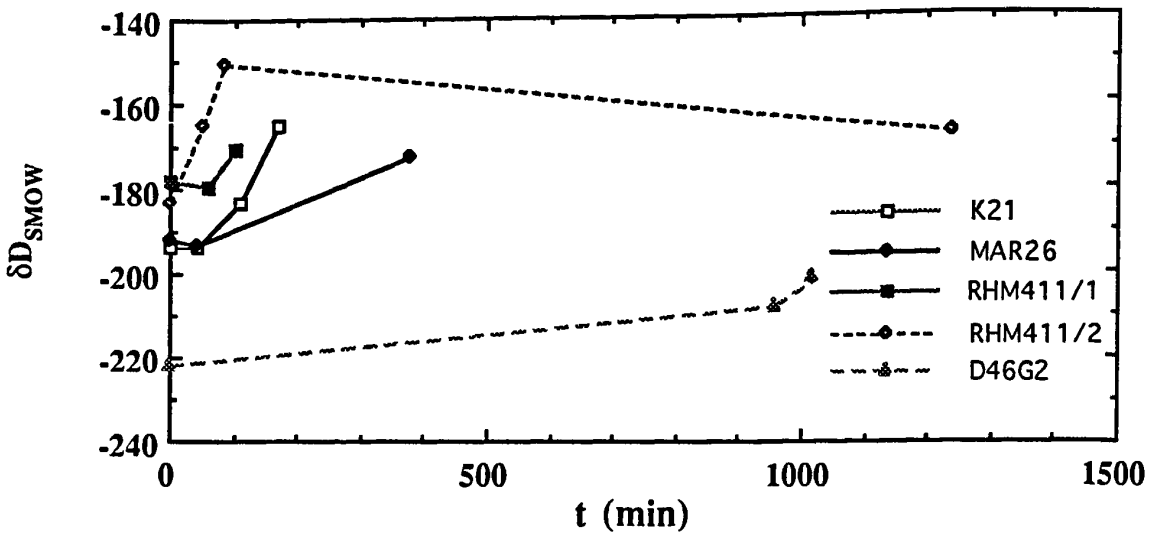


Figure 16. Relationship between δD of water released from laser ionization of various hydrous minerals, and the time (min) the samples were under vacuum in the sample chamber prior to analysis. Most of the subsequent analyses are closer to the conventionally determined values (become relatively enriched in D) as the time in vacuum increases.

samples is similar to that used for the hydrous silicate minerals. Because carnallite dehydrates in vacuum and halite may leak inclusion gases through fractures, the time an evaporite mineral is under vacuum prior to analysis was minimized.

Hydrogen released from fluid inclusions in halite and the structural water in carnallite using the Nd:YAG laser had yielded $\delta D$ values that were consistently depleted in D relative to conventionally determined values, similar to what was observed for the values of the hydrous silicates (Table 7/Fig. 17). Further, as $\delta D$ values from conventional analyses increase in value, differences between the values obtained from laser and conventional analyses also increase. This progressive divergence between $\delta D$ values determined by laser ionization and the true $\delta D$ values suggests the presence of a contaminant that has a low $\delta D$ value and similar concentration in each sample. As shown in Figure 17, the $\delta D$ value of this contaminant is near $-200^{\circ}/_{\circ\circ}$, where the line describing the values obtained with the laser and the real $\delta D$ values intersect. The most probable contaminant is adsorbed atmospheric water, having a low $\delta D$ value similar to that of local water vapour, on the surface of the minerals. Thus, the closer the isotopic composition of the structural water is to the composition of the contaminant water, the less the apparent disparity in the results between conventional and laser analyses. Some of the variations in the halite results

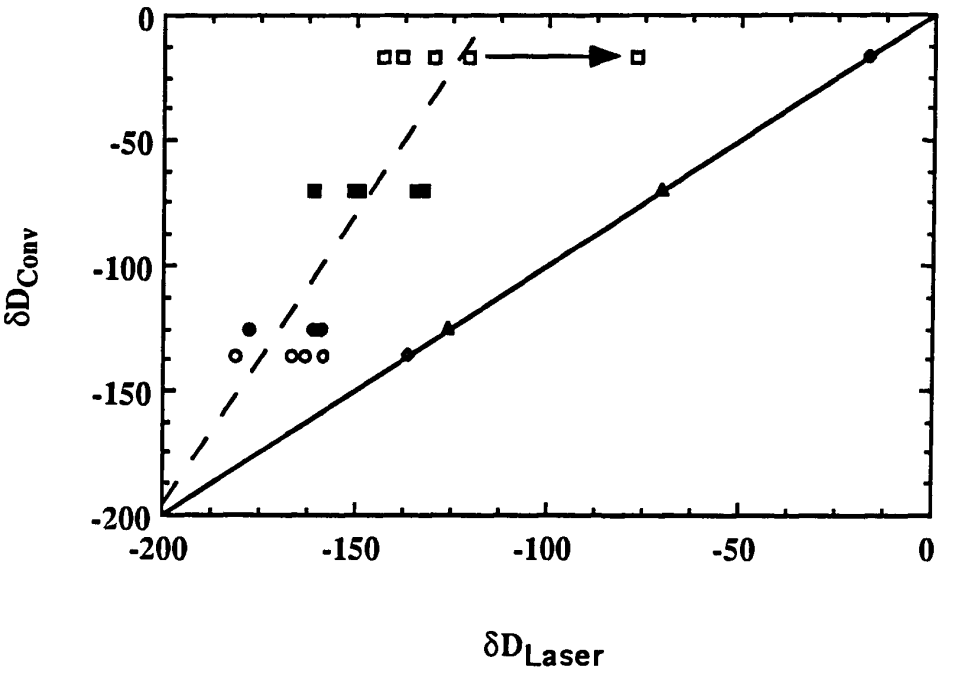


Figure 17. δD values of fluid inclusion-rich halite (SYN-B= ○ and SYN -D=□) and carnallite (BE503=■ and LPE2= ●) as determined by laser ionization ($\delta D_{laser}$) relative to the values determined conventionally ($\delta D_{corr}$). The best fit line of the laser data, intercepts the theoretical line demarking indentical $\delta D_{Conv}$ and $\delta D_{Laser}$ values at δD values near -200, which can be interpreted as the isotopic composition of absorbed water. The sample of SYN-D closest to the conventional values as indicated by the arrow was in vacuum for 12 hours before analysis whereas, all others were analyzed before 1 hour in vacuum.

are probably due to variability in the density of inclusions within a halite sample, thus changing the ratio of contaminant to inclusion water (Fig. 17).

Calculation of the expected yields of water from evaporite samples can be obtained by using the mass of the sample and the wt%$H_2O$ of the sample as determined by the conventional method. For example, BE503-1 with a mass of 38.81mg and 37.0wt%$H_2O$ should have produced approximately 770$\mu$moles of $H_2O$ if all of the water in the sample had been collected. 6.2$\mu$moles of $H_2O$ were recovered in the actual experiment. Similarly, halite sample SYN-D-1 with a mass of 16.64mg should have yielded 18$\mu$moles of $H_2O$ at 2.2 wt%$H_2O$, but the actual yield was 4.7$\mu$moles of $H_2O$. These data indicate that the recovery of $H_2O$ from evaporite mineral samples using laser ionization is poor based on estimates of expected yield.

### 4.1.5 Further Evidence for Contamination from Surface Adsorbed Water: Results from Laser-Assisted Analyses of Kaolinite and Olivine

A kaolinite pellet (K21X) was exposed for 72 hours to water having a $\delta$D value of +1000 °/₀₀. The pellet was analyzed with the laser system and the results are presented in Table 8. Analyses of the treated pellet (K21X) done within one hour in vacuum in the laser system were enriched in D by over 130°/₀₀ relative to previous laser analyses of a kaolinite

Table 8.

Laser-Assisted Analyses of Kaolinite and Olivine.

| Sample No. | L.E., Mode, Style | Time (mins) | Weight % $H_2O$ | Pulses | µmoles $H_2O$ (yield) | $\delta D_{Laser}$ | $\delta D_{Corr}$ |
|---|---|---|---|---|---|---|---|
| K21X-0(Std) | n.a. | n.a. | 10.70 | n.a. | n.a. | n.a. | -42 |
| K21X-1 | 60, Qsw, S.P. | 0 | 10.70 | 300 | 2.00 | -38 | -43 |
| K21X-2 | 60, Qsw, S.P. | 50 | 10.70 | 300 | 2.31 | -26 | -31 |
| K21X-3 | 60, Qsw, S.P. | 2902 | 10.70 | 300 | 1.54 | -110 | -120 |
| OL-1 | 60-Qsw/60-L.P., S.P. | 0 | (0.0) | 350/100 | 1.60 | -195 | -211 |

K21X= kaolinite sample pellet exposed to water with $\delta D_{SMOW}$=+1000; OL-1 = olivine sample containing no structural water; L.E.= lamp energy; Mode= laser operating mode; Style= ionization technique; Qsw= Q-switched mode; L.P.= long pulse mode; Time= time in mins between sample loading and analysis; S.P.= single pit; Pulses= total pulses Qsw/L.P. impinged onto the sample; $\delta D_{Laser}$= raw laser values; $\delta D_{Corr}$= corrected laser values; n.a.= not applicable; (Std)= isotopic composition determined by conventional technique.

pellet (K21) not exposed to the D-enriched water (Table 5), indicating the sample (K21X) had adsorbed some of the D-enriched water. Pellet K21X analyzed again after two days in vacuum produced much lower $\delta$D values that were closer to the original values determined by laser analysis of the untreated pellet (K21). The enrichment in D of the kaolinite pellet exposed to water having a $\delta$D value of +1000°/₀₀ is compatible with the interpretation that adsorbed atmospheric water can contaminate hydrous mineral samples.

This interpretation was further tested by determining the isotopic composition of surface adsorbed water on an anhydrous olivine grain. Olivine does not contain significant amounts of structural water or hydrogen. If there were a contribution of hydrogen from the olivine the volume, of material ionized with the laser is so small the contribution would be negligible, so that the majority of water released by laser ionization must be contaminant atmospheric water. The $\delta$D value of the olivine analyzed with the laser system was -211°/₀₀. As local meteoric water has a $\delta$D value of approximately -150°/₀₀ to -170°/₀₀ and local atmospheric water is likely to have a lower $\delta$D value, the water released from the olivine is compatible with the interpretation that adsorption of local meteoric water is a contaminant of all mineral samples.

## 4.2 Discussion of the Hydrous Mineral Results

The mineral ionization model developed to explain the carbonate data can be applied to the hydrous mineral data. However, due to the severity of the atmospheric water contamination problem hydrogen isotope fractionations related to the ionization process are difficult to discern.

### 4.2.1 Mineral Ionization Model

The initial excitation of the mineral by the laser energy (Stage 1) depends on the absorption characteristics of the sample (Fig. 12). The infrared spectra of various hydrous minerals, in the region of 1.0$\mu$m, show the same type of iron absorption effects as do the carbonate minerals, that is absorption of the energy from 1.0$\mu$m to 1.5$\mu$m (Fig. 18). The absorption effects and low efficiency of laser ionization for extraction of primary hydrogen from the mineral, as is shown from the evaporite mineral analyses and the yield estimates from ionization pit volumes, suggest that the $\delta$D value of the ion plume is likely fractionated from the $\delta$D value of the mineral similar to the carbonate analyses.

The formation of stable chemical phases during cooling of the ion plume (Stage 2) should control isotopic fractionations between different gas species (Fig. 12). During laser ionization of hydrous minerals, CuO at 500°C was needed to enhance yields, which is evidence that water is not the only hydrogenic gas species formed. Substantial differences,

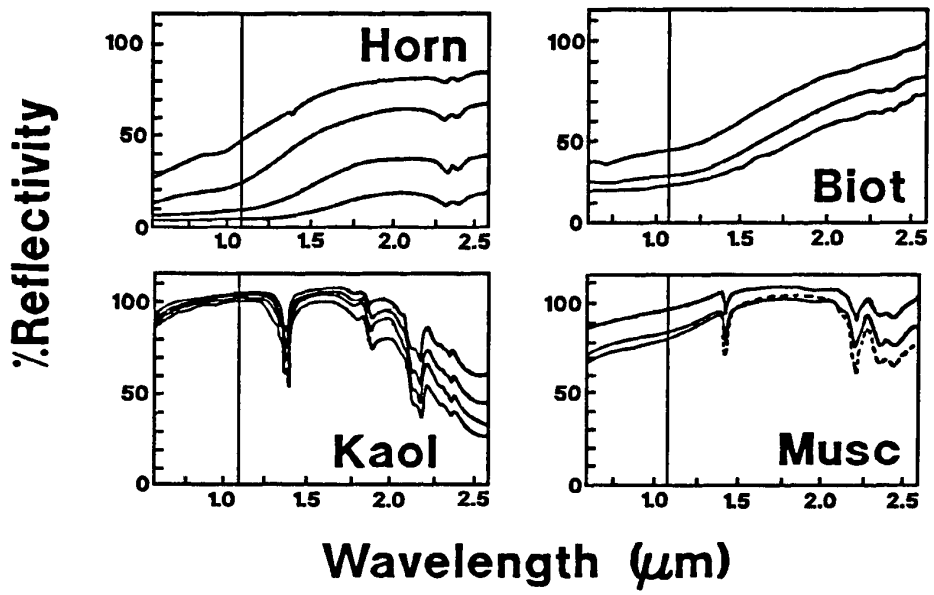


**Figure 18. Infrared spectra of hornblende, biotite, kaolinite, and muscovite in the region of the Nd:YAG laser wavelength (lines at 1.064 μm) showing the effect of Fe on the absorption characteristics of various hydrous silicates (after Hunt and Salisbury, 1970).**

commonly by up to 100°/oo, in the δD value determined by analysis of water without CuO relative to analysis of all hydrogenic gases with CuO suggest that fractionations among gases in the ion plume occur in much the same manner as was observed in the
carbonate results.

Although atmospheric water contamination is an obvious interference in laser extraction of hydrous minerals, it is possible that some chemical effects related to composition are being observed in the amphibole analyses. Amphibole D46G2 and RHM-409 have the same conventionally determined δD values, but repeated analysis of D46G2 and RHM-409 using laser ionization yield two distinct groups of δD values averaging to -218°/oo and -189°/oo, respectively. Several factors could contribute to this observed discrepancy including grain size, inclusions of different hydrous minerals, or differences in the water contents of the samples. However, sample D46G2 contains 23.53wt% FeO whereas RHM-409 is almost iron free (Table 4). This may be a case where differences in absorption of energy by the mineral affects hydrogen isotope fractionation between the plasma cloud and the sample due to differences in composition, specifically , the transition metal content of the sample, in the same way as was observed for the carbonates.

### 4.2.2 Contamination Effects

Laser analyses of hydrous minerals can be severely affected by the contribution of adsorbed atmospheric water onto the sample surface. This effect is observable in laser analyses of the fluid inclusion-rich halites and carnallites (Fig. 17), of the anhydrous olivine and the kaolinite (K21X) that adsorbed D-rich water (Table 8), in the overall consistent depletion of laser ionization results (Table 5), in the time-dependent changes in yields (Fig. 15) and isotopic compositions (Fig. 16).

Sample preheating to approximately 100°C, trichloroethane cleaning of sample surfaces, and attempts to raster away surface layers to, ideally, analyze pristine material deeper in the sample, all failed to remove the adsorbed component. More severe measures such as preheating at 300°C could work, but may affect the structural water in some samples as well. D/H analysis by ion probe (DeLoule et al., 1991) uses a liquid nitrogen trap to remove adsorbed water during bakeout at 120°C for at least three days in the ion probe. This method may be applicable for removing the adsorbed water from hydrous mineral samples for laser-assisted analysis.

Hydrous mineral contamination with local atmospheric water having a $\delta D$ value of approximately $-200^{\circ}/_{\circ\circ}$ is a difficult problem to correct because there are two isotopically distinct reservoirs of hydrogen in the sample. This problem is further complicated by factors such as the

water content and the absorption characteristics of the sample which will both affect the relative quantities of each reservoir released by the ionization process. Potential solutions include using laser operating conditions or laser wavelengths that do not liberate the adsorbed water, or to remove the adsorbed water using a method similar to DeLoule et al. (1991). Once the contaminant water has been eliminated correction factors may be calculated to correct for fractionations due to the ionization process.

## 5. SUGGESTIONS FOR FUTURE RESEARCH

To become a routine procedure for stable isotope analysis, laser extraction must approach the accuracy and precision of standard methods. All ordered crystalline substances have characteristic absorption and reflection spectral patterns across the entire spectrum of light from X-rays to radio waves. It is obvious from the research reported in this thesis that simply 'atomizing' mineral samples with high-energy laser photons will not produce unfractionated gases for isotopic analysis. For example, transition metal contents should not affect the ionization process, but do as has been shown for Nd:YAG laser extraction of carbonate minerals. Instead, the wavelength of laser energy should be such that absorption peaks associated with chemical bonds of the atoms to be analyzed are accessed. The most critical refinement that must be made to the system is the use of a tuneable laser so that fractionations between laser produced gases, such as CO and $CO_2$ or $H_2O$, and their respective samples can be minimized through manipulation of laser operating wavelengths to maximize absorption. Fractionations must also be quantified relative to the chemical composition of the sample, as has been done for sulphides (Kelley and Fallick, 1990; Crowe et al., 1990). Conceptually, it is important to use the laser energy to break the chemical bonds of the atoms to be measured for their isotopic ratios rather than simply providing generic high energy photons intending to break all

chemical bonds in the mineral.

## 6. CONCLUSIONS

A laser extraction system for isotopic analysis was developed and tested on various carbonate, hydrous silicate, and evaporite minerals at the University of Saskatchewan. The isotopic compositions of these minerals, determined using laser ionization, are variable and consistently different than compositions determined by conventional methods.

The results of carbonate analyses were used to develop a two-stage model to explain the variable yields and isotopic compositions of gases produced through laser ionization using a Nd:YAG laser. The ratio of $CO_2/CO$, the overall yield of gas per pulse, and the $\delta^{13}C$ and $\delta^{18}O$ values of combined CO and $CO_2$ are primarily controlled by photon absorption of the carbonate mineral (Stage 1). Carbonates with transition metal cations absorb laser photons more efficiently, yielding greater amounts of total gas and higher ratios of $CO_2/CO$ than other carbonates. The isotopic compositions of combined CO and $CO_2$ differ significantly from those obtained by conventional acid dissolution, and these differences are mineral specific and related to chemical composition. Fractionations occur through incomplete ionization of the carbonates and from formation of residual compounds which remain in the sample chamber. The isotopic data also show there are regular fractionations between CO and $CO_2$ independent of the carbonate mineral. These fractionations are attributable to a kinetically controlled process of stable gas formation as the ion plume

expands and cools, including interference from absorption of the laser beam by the plume (Stage 2).

There is limited application of this model to results of laser ionization of hydrous minerals because of overwhelming contamination by adsorbed atmospheric water. Experiments demonstrate that adsorbed atmospheric water on minerals is ubiquitous, and that the atmospheric water component has an isotopic composition commensurate with local meteoric water. Reduced yields and regular shifts in $\delta D$ values as a function of time in vacuum suggest that the contribution of contaminant atmospheric water can be diminished, but not completely removed from the samples with the present system.

In situ laser-assisted extraction for isotopic analyses of minerals is a major advance in the study of the nature of geologic processes by allowing fine-scale stable isotopic determinations in concert with petrographic relationships. This research has attempted to provide a fundamental understanding of the behaviour of laser-mineral and laser-plasma-mineral interactions that will lead to further technical advancements in the application of laser-based analytical methods to geological studies.

## 7. REFERENCES

Aggett, J., Burton, C. A., Lewis, T. A., Llewellyn, D. R., O'Connor, C. and Odell, A. L., 1965. The isotopic analysis of oxygen in inorganic compounds and in coordination compounds containing organic hazards. Internat. J. Applied Radiat. Isotopes, 16: 165-170.

Baertschi, P. and Silverman, S. R., 1951. The determination of relative abundances of the oxygen isotopes in silicate rocks. Geochim. Cosmochim. Acta, 1: 317-328.

Bigeleisen, J., Pearlman, M. L., and Prosser, H. C., 1952. Conversion of hydrogenic materials to hydrogen for isotopic analysis. Anal. Chem., 24: 1356-1357.

Borthwick, J. and Harmon, R. S., 1982. A note regarding $ClF_3$ as an alternative to $BrF_5$ for oxygen isotopic analysis. Geochim. Cosmochim. Acta, 46: 1665-1668.

Carpenter, S. J. and Lohmann, K. C., 1989. $\delta^{18}O$ and $\delta^{13}C$ variations in late Devonian marine cements from the Golden Spike and Nevis reefs, Alberta, Canada. J. Sed. Pet., 59: 792-814.

Clayton, R. N. and Mayeda, T. K., 1963. The use of bromine pentafluoride in the extraction of oxygen from oxides and silicates for isotopic analysis. Geochim. Cosmochim. Acta, 27: 43-52.

Crowe, D. E., Valley, J. W. and Baker, K. L., 1990. Micro-analysis of sulphur-isotope ratios and zonation by laser microprobe. Geochim. Cosmochim. Acta, 54: 2075-2092.

Dalrymple, G. B., 1987. Continuous laser dating system (abs). Branch of Isotope Geology, U. S. Geologic Survey, Menlo Park, CA.

Dalrymple, G. B., 1989. The GLM continuous laser system for $^{40}Ar/^{39}Ar$ dating:description and performance characteristics. In: W. C. Shanks and R. E. Criss (Editors), New Frontiers in Stable Isotopic Research: Laser Probes, Ion Probes, and Small Sample Analysis. U. S. Geol. Surv. Bull., 1890, pp. 174.

DeLoule, E., France-Lanord, C., and Albarede, F., 1991. D/H analysis of minerals by ion probe. In: H. P. Taylor, J. R. O'Neil, and I. R. Kaplan (Editors), A Tribute to Samuel Epstein. The Geochemical Soc., Special Publication No. 3: 53-62.

Dickson, J. A. D., 1991. Disequilibrium carbon and oxygen isotope variations in natural calcite. Nature, 353: 842-844.

Dickson, J. A. D., Smalley, P. C., Raheim, A., and Stijfhoorn, D. E., 1990. Intracrystalline carbon and oxygen isotope variations in calcite revealed by laser microsampling. Geology 18: 809-811.

Dickson, J. A. D., Smalley, P. C., and Kirkland, B. L., 1991. Carbon and Oxygen isotopes in Pennsylvanian biogenic and abiogenic aragonite (Otero County, New Mexico): A laser microprobe study. Geochim Cosmochim Acta, 55: 2607-2613.

Farmer, V. C. (Editor), 1974. The Infrared Spectra of Minerals. Bartholomew Press, Dorking, Surrey, pp. 539.

Franchi, I. A., Boyd, S. R., Wright, I. P. and Pillinger, C. T., 1989. Application of lasers in small-sample stable isotopic analysis. In: W. C. Shanks and R. E. Criss (Editors), New Frontiers in Stable Isotopic Research: Laser Probes, Ion Probes, and Small Sample Analysis. U. S. Geol. Surv. Bull., 1890, pp. 174.

Franchi, I. A., Wright, I. P., Gibson, E. K., Jr. and Pillinger, C. T., 1986. The laser microprobe: a technique for extracting carbon, nitrogen, and oxygen from solid samples for isotopic measurements. J. Geophys. Res., 91(B4): D514-D524.

Friedman, I. and Smith, R. L., 1958. The deuterium content of water in some volcanic glasses. Geochim. Cosmochim. Acta, 15: 218-228.

Hunt, G. R. and Salisbury, J. W., 1970. Visible and near-infrared spectra of minerals and rocks: I silicate minerals. Mod. Geol., 1: 283-300.

Hunt, G. R. and Salisbury, J. W., 1971. Visible and near-infrared spectra of minerals and rocks: II carbonates. Mod. Geol., 2: 23-30.

Jones, L. M., Taylor, A. R., Winter, D. L., Hunt, S. P. and Keen, G. W., 1986. The use of the laser microprobe for preparation in stable isotope mass spectroscopy (abs). Terra Cognita, 6(2): 263.

Kelley, S. P. and Fallick, A. E., 1990. High precision spatially resolved analysis of $\delta^{34}S$ in sulphides using a laser extraction technique. Geochim. Cosmochim. Acta, 54: 883-888.

Killingley, J. S. and Berger, W. H., 1979. Stable isotopes in a mollusc shell: Detection of upwelling events. Science, 205: 186-188.

Kyser, T. K. and O'Neil, J. R., 1984. Hydrogen isotope systematics of submarine basalts. Geochim. Cosmochim. Acta, 48: 2123-2133.

Longinelli, A. and Craig, H., 1967. Oxygen-18 variations in sulphate ions in sea water and saline lakes. Science, 156: 56-59.

McCrea, J. M., 1950. On the isotope chemistry of carbonates and a paleo-temperature scale. J. Chem. Phys., 18: 849-857.

Mattey, D. P., Macpherson, C. G., and Harris, J., 1992. Oxygen isotope analysis of syngenetic inclusions in diamond by laser microprobe (abs). E. O. S. Trans., 73(14): 336.

Megrue, G. H., 1967. Isotope analysis of rare gases with a laser microprobe. Science, 157: 1555-1557.

Muhs, D. R. and Kyser, T. K., 1987. Stable isotope compositions of fossil molluscs from southern California: Evidence for a cool last interglacial ocean. Geology, 15: 119-122.

Powell M. D. and Kyser T. K., 1991. Analysis of $\delta^{13}C$ and $\delta^{18}O$ in calcite, dolomite, rhodochrosite, and siderite using a laser extraction system. Chem. Geol.(Isot. Geosci. Sect.) 94: 55-66.

Powell M. D. and Kyser T. K., 1991. Laser decrepitation of aqueous fluid inclusions in halite for determination of D/H ratios (abstr.) G.A.C.-M.A.C., 16: A101.

Rafter, T. A., 1965. Recent sulphur isotope measurements on a variety of specimens examined in New Zealand. Bull. Volcanology, 28: 3-20.

Richet, P., Bottinga, Y., and Javoy, M., 1977. A review of hydrogen, carbon, nitrogen, oxygen, sulphur, and chlorine stable isotope fractionation among gaseous molecules. Ann. Rev. Earth Planet Sci., 5: 65-110.

Sharp, Z. D., 1990. A laser-based microanalytical method for the In-Situ determination of oxygen isotope ratios of silicates and oxides. Geochim. Cosmochim. Acta, 54: 1353-1357.

Sharp, Z. D., 1992. In situ laser microprobe techniques for stable isotope analysis. In: R. S. Harmon and R. W. Hinton (Editors), Frontiers in Isotope Geosciences. Chem. Geol. (Isot. Geosci. Sect.), 101: 3-19.

Smalley, P. C., Maile, C. N., Coleman, M. L., and Rouse, J. E., 1992. LASSIE (laser ablation sampler for stable isotope extraction) applied to carbonate minerals. Chem. Geol. (Isot. Geosci. Sect.) 101: 43-52.

Smalley, P. C., Stijfhoorn, D. E., Raheim, A., Johansen, H. and Dickson, J. A. D., 1989. The laser microprobe and its application to the study of C and O isotopes in calcite and aragonite. Sed. Geol., 65: 211-221.

Sommer, M. A., Yonover, R. N., Bourcier, W. L., and Gibson, E. K., 1985. Determination of $H_2O$ and $CO_2$ concentrations in fluid inclusions in minerals using laser decrepitation and capacitance manometer analysis. Anal. Chem., 57: 449-453.

Svelto, O. and Hanna, D. C. (translation), 1982. Principles of Lasers. 2nd. Ed. Plenum Press, New York, pp. 375.